

Extracellular matrix molecules and synaptic plasticity: immunomapping of intracellular and secreted Reelin in the adult rat brain

Tania Ramos-Moreno, María J. Galazo, Cesar Porrero, Verónica Martínez-Cerdeño and Francisco Clascá

Department of Anatomy & Neuroscience, School of Medicine, Autónoma University, Ave. Arzobispo Morcillo s/n., Madrid 28029, Spain

Keywords: ApoE 2 receptors, cerebral cortex, dendritic spines, NMDA receptor, VLDL receptors

Abstract

Reelin, a large extracellular matrix glycoprotein, is secreted by several neuron populations in the developing and adult rodent brain. Secreted Reelin triggers a complex signaling pathway by binding lipoprotein and integrin membrane receptors in target cells. Reelin signaling regulates migration and dendritic growth in developing neurons, while it can modulate synaptic plasticity in adult neurons. To identify which adult neural circuits can be modulated by Reelin-mediated signaling, we systematically mapped the distribution of Reelin in adult rat brain using sensitive immunolabeling techniques. Results show that the distribution of intracellular and secreted Reelin is both very widespread and specific. Some interneuron and projection neuron populations in the cerebral cortex contain Reelin. Numerous striatal neurons are weakly immunoreactive for Reelin and these cells are preferentially located in striosomes. Some thalamic nuclei contain Reelin-immunoreactive cells. Double-immunolabeling for GABA and Reelin reveals that the Reelin-immunoreactive cells in the visual thalamus are the intrinsic thalamic interneurons. High local concentrations of extracellular Reelin selectively outline several dendrite spine-rich neuropils. Together with previous mRNA data, our observations suggest abundant axoplasmic transport and secretion in pathways such as the retino-collicular tract, the entorhino-hippocampal ('perforant') path, the lateral olfactory tract or the parallel fiber system of the cerebellum. A preferential secretion of Reelin in these neuropils is consistent with reports of rapid, activity-induced structural changes in adult brain circuits.

Introduction

Extracellular matrix (ECM) molecules interact with each other and with cell-surface receptors, modifying adhesive forces and/or signaling cues that are critical for correct cell proliferation, migration or differentiation during brain development. Moreover, many of these ECM molecules remain widely and selectively distributed in the adult brain. Their known ability for cell signaling and for adhesion regulation make them potential modulators of synaptic plasticity (Dityatev & Schachner, 2003; Berardi *et al.*, 2004).

Evidence for such a role is now firmly established for the ECM glycoprotein Reelin (D'Arcangelo, 2005a). By binding to lipoprotein receptors, Reelin can activate a complex signaling cascade that exerts a robust effect on long-term potentiation in the hippocampus (Weeber *et al.*, 2002). This effect involves modulation of the *N*-methyl-D-aspartate receptor (NMDAR), a key molecular switch for activity-induced synaptic changes (Beffert *et al.*, 2005; Chen *et al.*, 2005; Sinagra *et al.*, 2005). In addition, Reelin is well known as a crucial regulatory signal for the migration and/or dendritic growth of some developing (Tissir & Goffinet, 2003; Jossin, 2004; Niu *et al.*, 2004; D'Arcangelo, 2005b) and stem-cell-derived adult neuron populations (Hack *et al.*, 2002; Haas *et al.*, 2002). Because these effects involve regulation of cell adhesion and/or cytoskeletal

dynamics, there have been suggestions that, similarly, Reelin might influence local cell adhesion or motility in adult synapses (Impagnatello *et al.*, 1998; Rodríguez *et al.*, 2000; Quattrocchi *et al.*, 2002).

A large molecule (~400 kDa), Reelin is constitutively secreted by neurons (Lacor *et al.*, 2000; Derer *et al.*, 2001). In adult mammals, several brain neuron populations express Reelin (Ikeda & Terashima, 1997; Alcántara *et al.*, 1998; Pesold *et al.*, 1998). In these neurons, immunolabeling studies have located Reelin within secretory organelles (Pappas *et al.*, 2001; Martínez-Cerdeño *et al.*, 2002) or as intraxonal particles (Martínez-Cerdeño *et al.*, 2003; Pappas *et al.*, 2003). In addition, secreted Reelin accumulates extracellularly in some neuropil areas (Miyata *et al.*, 1996; Pesold *et al.*, 1998; Pappas *et al.*, 2001; Pérez-García *et al.*, 2001; Misaki *et al.*, 2004), and can associate with integrin receptors at perisynaptic sites (Rodríguez *et al.*, 2000).

In previous immunolabeling studies in adult non-human primates and carnivores (Martínez-Cerdeño *et al.*, 2002, 2003), we observed major interspecies differences. We wished to compare our findings with equivalent data in rodents, for which *in situ* mRNA hybridization (ISH) data were available (Ikeda & Terashima, 1997; Alcántara *et al.*, 1998; Pesold *et al.*, 1998; Haas *et al.*, 2000). However, the published adult rodent immunolabeling data (Miyata *et al.*, 1996; Pesold *et al.*, 1998, 1999; Pérez-García *et al.*, 2001; Misaki *et al.*, 2004) were limited and fragmentary. The mRNA data were insufficient to establish the location of the protein because, after translation, Reelin may undergo axonal transport (Pesold *et al.*, 1998; Derer *et al.*, 2001), secretion (D'Arcangelo *et al.*, 1997), dimerization (Benhayon *et al.*,

Correspondence: Dr F. Clascá, as above.
E-mail: francisco.clasca@uam.es

Received 23 August 2005, revised 28 October 2005, accepted 23 November 2005

2003; Strasser *et al.*, 2004), cleavage (Jossin, 2004) and even internalization by other cells (D'Arcangelo *et al.*, 1999; Morimura *et al.*, 2005). Thus, we decided to undertake a systematic immunomapping of Reelin protein in adult rats.

Materials and methods

Brain tissue from 13 adult (2–14 months of age) Sprague–Dawley rats of either sex was used. Procedures were carried out in accordance with European Community Council Directive 86/609/EEC and approved by our University's Bioethics Committee.

In the course of the project, we tried several modifications of the fixation and immunostaining protocols; for brevity, only the procedure that we found consistently to give the best results, which are the basis for the reported data and illustrations, is described below. Animals were killed with an intraperitoneal overdose of sodium pentobarbital (80 mg/kg), and perfused through the heart with saline (5 min), followed by cold (4 °C) 4% paraformaldehyde in 0.1 M phosphate buffer (PB) for 45 min. Subsequently, brains were blocked in the stereotactic coronal plane, removed from the skull and soaked in 30% sucrose in PB at 4 °C for 48 h. Serial 40- μ m-thick coronal sections were obtained on a Leica freezing microtome. To examine the retinas, the eyes of two animals were also removed, cryoprotected as described and freeze-sectioned at 50 μ m perpendicular to the iris.

Immunolabeling and controls

Series of sections sampling the various brain regions along the rostrocaudal axis were used for Reelin immunodetection. Endogenous peroxidase was quenched by 20 min incubation in 1% H₂O₂ in phosphate-buffered saline (PBS). Subsequently, sections were pre-incubated, free-floating, in 0.1 M citrate buffer pH 6.0 at 90 °C for 10 min (Shi *et al.*, 2001). Note that we used lower temperatures and shorter times than for standard heat-induced antigen retrieval protocols.

To rule out the possibility of non-specific labeling, parallel series of tissue sections were assayed with three different, well-characterized monoclonal antibodies that bind non-overlapping amino acid sequences near the Reelin N-terminus (D'Arcangelo *et al.*, 1997; de Bergeyck *et al.*, 1998). This protein region is present in the full-length Reelin as well as in some of the biologically active fragments in which the full-length form of Reelin is cleaved after secretion (Lambert de Rouvroit *et al.*, 1999; Jossin *et al.*, 2004). The antibodies used were 142 (1 : 400–1 : 1000, Calbiochem, San Diego, CA, USA), CR50 (1 : 100; a gift from Dr Masaharu Ogawa, Riken, Japan) or G10 (1 : 400, Chemicon, Temecula, CA, USA). Sections were incubated overnight at room temperature in a medium containing an anti-Reelin antibody + 3.3% normal rabbit serum + 1% bovine serum albumin (Sigma, St Louis, MO, USA) + 0.3% Triton X-100 in PBS. Immunolabeling was revealed using biotinylated rabbit anti-mouse serum (2 h, Sigma) and then the avidin-biotinylated horseradish peroxidase complex (Vector Laboratories, Burlingame, CA, USA) for 1.5 h, followed by a peroxidase reaction (0.001% H₂O₂ in cold PBS, 3–15 min) using diaminobenzidine (DAB) as the chromogen. Multiple rinses in PBS were intercalated between each step. The labeling yielded by the three antibodies was consistent in all brain regions (see Supplementary material, Figs S1 and S2). In the remaining figures, antibody 142 was applied. Throughout the study, we did not use metal enhancement of the DAB labeling so as to prevent the risk of spurious metal impregnation.

The coincident results from three different, well-characterized monoclonal antibodies virtually ruled out non-specific immunostain-

ing. Nevertheless, we ran multiple additional controls for labeling specificity (see supplementary Fig. S1). First, we either omitted the primary antibody or substituted it with non-immune mouse serum (Vector Laboratories). Both assays left the nervous tissue unlabeled, but produced some staining in pia mater, blood vessels and in a few ependymal cells. This observation suggests that the labeling in these structures could be, at least in part, non-specific; thus, we do not describe it in the following text. Second, we pre-absorbed the primary antibodies with the supernatant obtained from a culture of EBNA-293 cells that had been transfected with a Reelin cDNA expression vector (PCDNA3, gift from Dr J. A. del Rio, Science Park, Barcelona University, Spain). The supernatant was collected 4 days after lipofectamine transfection and concentrated 50 times using a Centricon-20 centrifuge (mol. wt 100 kDa, Amicon, Millipore, Billerica, MA, USA). Incubation with the primary antibodies mixed with this supernatant yielded no labeling, whereas a parallel negative control run with primary antibodies mixed with a concentrated supernatant from parallel mock-transfected cells produced normal labeling. Third, to rule out the possibility that some of our labeling might correspond to avidin binding to endogenous biotin (McKay *et al.*, 2004), or a spurious cross-reaction of the secondary rabbit antiserum, we conducted parallel assays applying 2-h incubations in ABC at room temperature, which yielded no labeling, or substituting the biotinylated secondary antiserum with an Alexa 568-conjugated goat antiserum (Molecular Probes, Eugene, OR, USA), which produced a fluorescent labeling identical to that observed in the standard experiments.

Western blotting

To ascertain further immunolabeling specificity in brain regions such as the striatum and dorsal thalamus, where ISH studies had not reported labeling, we carried out a Western blot analysis with tissue sampled from these regions (see Supplementary material, Fig. S2). As control, we also Western-blotted lysate from parietal isocortex, a region where our protein data were basically in agreement with published mRNA data (Alcántara *et al.*, 1998). For this experiment, we perfused two additional adult rats with sterile saline for 5 min, to remove blood (low levels of Reelin are present in blood, Smalheiser *et al.*, 2000), then extracted the brain from the skull and sectioned it into 0.5-mm-thick coronal slices. Under the dissecting microscope, we sampled tissue from the lateral posterior nucleus of the thalamus and from the caudate-putamen. Other samples were taken from the parietal isocortex. One milliliter of lysis buffer was added to each sample, and the mix was mechanically homogenized and heat-denatured. Subsequently, lysate samples (30 μ L striatum, 30 μ L thalamus, and 10 μ L parietal cortex) were analysed in parallel lanes on 3% and 5% sodium dodecyl sulfate-polyacrylamide electrophoresis gels, first at 75 mV for 10 min and then at 150 mV for 65 min. Molecular weight standards were run in additional lanes. The separated proteins were electroblotted at 150 mA overnight at 4 °C onto a Protran nitrocellulose membrane (Scheleicher & Schuell, Dassel, Germany) using a Mini-TransBlot system (Bio-Rad, Hercules, CA, USA). Non-specific binding was blocked by incubating in 10% milk powder in TRIS-saline buffer containing 0.4% Tween-20 (TBST) for 2 h. Blots were then incubated in agitation with the 142 monoclonal anti-RELN antibody diluted 1 : 400 in TBST. After repeated washing in TBST, the blots were incubated for 1 h in anti-mouse antibody and peroxidase-labeled goat serum (Bio-Rad, 1 : 10 000 dilution). Staining was visualized with a rapid electrochemoluminescent detection system (ECL Western Blotting System, Amersham, Piscataway, NJ, USA) and exposed to Hyperfilm-ECL (Konica-Minolta).

Some sections were counterstained with Thionin to define accurately the position of the labeled neurons and their relationship to other unlabeled cells. Likewise, retinal cytoarchitecture was delineated on 1- μ m semithin sections taken from the 50- μ m-thick eye sections, after dehydration, inclusion in Araldite and staining with Toluidine blue.

Immunolabeling co-localization

In some experiments, parallel sections were immunostained with an antibody against mouse anti-neuronal nuclei antigen (NeuN, 1 : 400; Chemicon) as an additional, more precise cytoarchitectonic reference of neuron number and distribution. In other experiments we wanted to examine the possible correlation between the distribution of Reelin-immunoreactive (ReIn-ir) neuronal somata and the striosomal compartment of the caudate-putamen. To this end, sections adjacent to those labeled with anti-Reelin antibodies were assayed with a monoclonal antibody against the μ -opioid receptor (1 : 400; DiaSorin, Saluggia, Italy) as a selective marker for the striosome compartment in rats (Prensa & Parent, 2001).

In a further group of experiments, tissue sections from two animals were double-labeled using antibodies against either Reelin or gamma-aminobutyric acid (GABA). These sections were obtained from two animals perfused with 2% paraformaldehyde + 0.2% glutaraldehyde in PB; their brains were sectioned as described above. Tissue sections were incubated in a solution that contained mouse monoclonal anti-Reelin 142 (1 : 400) and a rabbit polyclonal GABA antiserum (1 : 500; Sigma), as well as normal goat serum and bovine serum albumin. The primary antibodies were tagged either with an Alexa 568-conjugated goat anti-rabbit serum (1 : 100) or Alexa 488-conjugated goat anti-mouse serum (1 : 100; both from Molecular Probes). In all experiments, sections were finally mounted on glass slides, air-dried, dehydrated and coverslipped with DePeX.

Analysis and imaging

Tissue analysis was conducted under a Nikon 600 Eclipse microscope. Images were acquired with 100 \times plan-apochromatic objectives using a Nikon DMX 1200 digital camera in a single focal plane; depth-of-field enhancing algorithms were not used. Panoramic, high-resolution tissue images were produced as composites from serial 100 \times images taken using a precision motorized stage (Prior Scientific Instruments, Cambridge UK) driven by the AnalySIS image software package (Soft Imaging Systems, Münster, Germany). Canvas software (v.9, ACD Systems, Saanichton, BC, Canada) was employed for image processing and final figure composition on Apple G4 computers. Image processing consisted only of adjustments in tone scale and gamma, as needed to obtain optimal images. Local retouching was limited to areas outside the nervous tissue. We followed Paxinos & Watson's (1998) rat brain atlas to delineate brain structures and for anatomical nomenclature.

Co-localization tissue analysis in the double-labeling experiments was carried out with a Leica TCS SPII spectral confocal microscope sequentially applying argon (488 nm) and helium-neon (543 nm) laser lines, with dichroic mirror adjustments at 500 and 700 nm, respectively, to ensure complete channel separation. Serial 1- μ m-thick optical slices were taken on the z-axis. Co-localization analysis was carried out on 361 \times 361- μ m fields from the nuclei of interest. Confocal analysis revealed that, owing to the incomplete penetration of the GABA antibody through the thickness of the tissue section, GABA labeling was limited to the outer 4–5 μ m. Thus, we limited our

co-localization analysis to single 1- μ m optical slices taken near the surface in order to avoid underestimating GABA immunolabeling. Co-localization of Reelin and GABA signals was determined by computerized analysis of the fluorescence intensities in each image pixel using the Leica SPII Confocal software. Proportions of GABA-only, Reelin-only and double-labeled cell profiles were computed as a percentage of the total number of Reelin-labeled cells counted. We made no attempt to estimate absolute cell numbers.

Results

The three anti-Reelin monoclonal antibodies applied on adjacent tissue sections yielded strictly coincident labeling patterns. The labeling delineated discrete cellular structures such as some neuronal somata, their proximal dendrites and initial axon segments. In addition, several gray matter regions showed a prominent homogeneous staining that we interpret as ECM labeling. Although the white matter was essentially labeling-free, some particular axonal tracts showed weak Reelin immunoreactivity as well. Overall, staining intensity varied markedly between the different cell populations and neuropil areas, suggesting substantial differences in protein content. Parallel control experiments (see Methods and Supplementary Material) showed that labeling of the pia mater, blood vessel walls and some ependymal cells was non-specific; thus, we do not describe this labeling in the following text.

ReIn-ir neuronal somata were numerous in the forebrain, mesencephalon and cerebellar cortex, whereas the pons and medulla contained markedly fewer ReIn-ir cells. At high magnification, neuronal somata labeling was always absent from the cell nucleus, indicating an intracytoplasmic location. The basic appearance and distribution of the labeling at high magnification was similar in weakly and heavily labeled cells. At high magnification, the labeling was uneven, mostly appearing as discrete beaded or elongated lump-like structures that usually grouped at the base of dendrites or of the axon. These ReIn-ir structures usually extended into the proximal dendrites. In some heavily labeled neurons, the individual axons were also visible at high magnification as a discontinuous line of very small (< 1 μ m) immunoreactive beads (Fig. 1C). The appearance of these beads under the light microscope is consistent with that of the secretory vesicles (Cameron *et al.*, 1993; Derer *et al.*, 2001).

Tables 1 and 2 provide a comprehensive account of our observations on the distribution of the cell somata, axons and neuropil labeling throughout the brain. The actual appearance of the ReIn-ir structures is documented in the figures. Therefore, the following text details only the most salient features of the labeling.

Reelin immunoreactivity in the olfactory bulb and olfactory areas

Four distinct neuron types in the main olfactory bulb (MOB) were ReIn-ir: the mitral and the tufted cells, all of which were labeled, a subpopulation of periglomerular cells and a subpopulation of granular cells (Fig. 1A–C). In addition, a few large cells scattered in the granular layer, presumably Cajal cells, were ReIn-ir. The labeling of mitral and tufted cells was heavy and revealed the somata, proximal dendrites and axons of these cells (Fig. 1B and C). Axonal labeling consisted of discrete, bead-like lumps that were clearly visible only at high magnification (Fig. 1C, arrowheads) and could be followed stretching through the deep MOB layers to join the lateral olfactory tract (LOT). As indicated above, this type of labeling is consistent with labeling of intra-axonal immunoreactive organelles. At low magnification, this axonal labeling was not clearly visible; instead, a faint

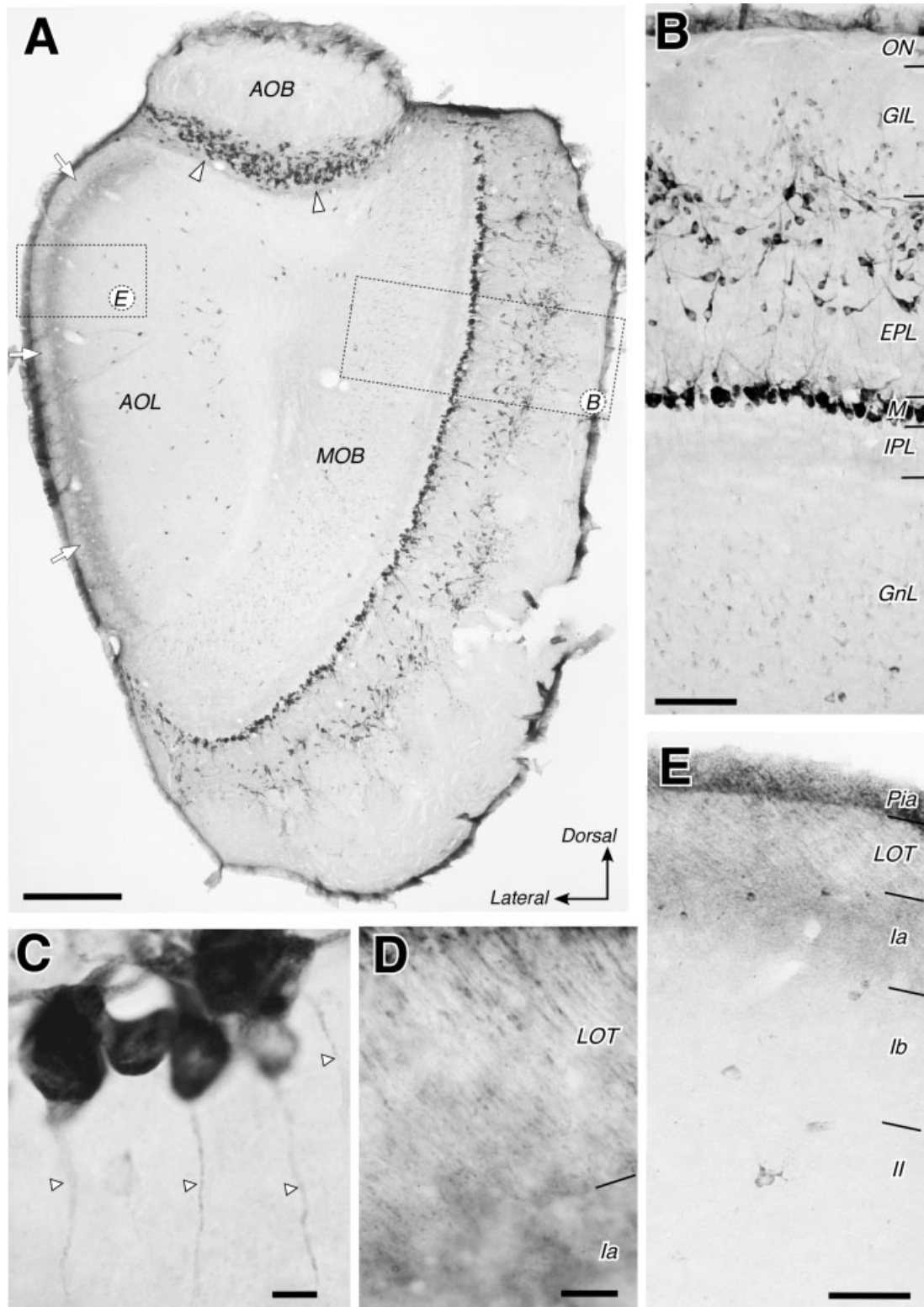


FIG. 1. Reelin-like immunolabeling in the olfactory bulb. (A) Panoramic view of a coronal section which encompasses the main (MOB) and accessory (AOB) olfactory bulbs, as well the lateral division of the anterior olfactory nucleus (AOL). Note the highly selective localization of labeling to particular cell layers and/or neuropil zones in each of these three fields. Arrows point to location of the lateral olfactory tract (LOT), while the arrowheads indicate the position of the internal plexiform layers in MOB. (B) Detail of the labeling in MOB (inset in A). Note that virtually all the mitral and tufted cells are heavily ReIn-ir. In addition, subpopulations of smaller periglomerular cells in the glomerular layer (GL) and of granular cells in the granular layer (GnL) are also immunoreactive. (C) High-magnification views of labeled mitral neurons in MOB. Note that, in addition to somata and dendrites, ReIn-ir is clearly visible in the axon of these cells (arrowheads). (D) Particulate labeling in the LOT axons and amorphous, presumably extracellular, labeling in sublayer Ia of AOL. The pial surface is at the top. (E) Labeling in the superficial layers of AOL (inset in A). Note the amorphous appearance of the immunoprecipitate in the superficial part of layer I (sublayer Ia), which we interpret as extracellular matrix labeling. The myelinated axon trunks in LOT also show immunoreactivity, although less heavily. Isolated ReIn-ir cell somata are present in these deep layers. For other abbreviations, see List. Scale bars, 500 μ m (A); 100 μ m (B and E); 10 μ m (C and D).

TABLE 1. Localization and relative proportions of Reelin-immunoreactive neuronal somata and neuropil in the rat telencephalon

	Neuronal somata	Neuropil /axons
Olfactory bulb		
Main olfactory bulb		
Glomerular layer (periglomerular cells)	○○○	+
Superficial plexiform layer (tufted cells)	●●	+
Mitral cell layer	●●●	+
Inner plexiform layer	-	+
Granular layer	○	+
Lateral olfactory tract	-	+++
Accessory olfactory bulb	●●●	+
Olfactory cortical areas		
Anterior olfactory nucleus		
Molecular layer	○	+++
Pyramidal layer	○	-
Multiform layer	○	+
Endopyriform nucleus	○	+
Olfactory tubercle	-	+++
Nucleus of the lateral olfactory tract	○	+
Pyriform cortex		
Molecular layer	●	+++
Pyramidal layer	●○	-
Polymorph layer	○	+
Other basal telencephalic regions		
Preoptic areas	●○○	++
Septo-hippocampal junction	○	+
Diagonal band nuclei	●○	+
Septal nuclei		
Medial	●○	++
Lateral ventral	○○	+
Other	○	+
Substantia innominata/anterior amigdaloid areas	●○	+
Ventral pallidum	-	-
Bed nucleus of stria terminalis	○	+
Stria terminalis (tract and nucleus)	○	+
Globus pallidus	○	-
Striatum	○○	+
Amygdaloid complex		
Corticomedial group	●○	+++
Basolateral group	○○	-
Central nuclei	○	-
Dorsal claustrum + endopyriform nucleus	○○	+
Hippocampal formation and parahippocampal cortex		
Fascia dentata		
Stratum moleculare	●	+++
Stratum granulare	-	-
Hilus	●●○	+
Cornu Amonnis		
Stratum lacunosum-moleculare	●●	+++
Stratum radiatum	●	+
Stratum pyramidale	-	-
Stratum oriens	●●	+
Alveus	-	-
Subicular complex		
Stratum moleculare	●	++
Stratum pyramidale	○○	+
Stratum oriens	○	+
Entorhinal cortex		
Layer I	●	+++
Layer II	●●●	+
Layer III	●○○	+
Layer IV	○○	+
Layer V	○	+
White matter (interstitial cells)	●	-
Isocortex		
Layer I	●●●	+++
Layer II	●	+
Layer III	●○	+

TABLE 1. Continued

	Neuronal somata	Neuropil /axons
Layer IV	●	+
Layer V	●●○	+
Layer VI	●○	+
White matter (interstitial cells)	●	-

For descriptive purposes only, labeled neuronal somata containing heavy, solid immunoprecipitate (filled circles) and those displaying a less heavy labeling (open circles) are distinguished. The number of circles represents a gross approximation of the relative number of each type of immunoreactive somata in a nucleus or layer (-, none detected; 1 circle, occasional isolated cells; 2 circles: numerous cells; 3 circles: all, or nearly all, the neurons are labeled). Likewise, crosses are used to represent differences in the density of neuropil/axonal immunoreactivity (-, none detected; +, faint labeling; ++, dense labeling; +++, very heavy labeling).

staining could be observed in the LOT. In addition, light neuropil labeling was evident in all cell layers of the MOB, but most particularly in the internal plexiform layer (IPL) (Fig. 1B).

All the mitral cells in the accessory olfactory bulb (AOB) were ReIn-ir. A band of heavy neuropil labeling delineated the IPL (Fig. 1A, arrowheads).

Figure 1 illustrates the labeling in the lateral division of the anterior olfactory nucleus (AOL): labeling was similar in the other divisions of the anterior olfactory nucleus. Isolated, weakly ReIn-ir neurons were present in all layers, but particularly in layer III, and they displayed fusiform or multipolar somata. The pyramidal cells of layer II were unlabeled. The myelinated LOT axons showed a faint labeling that, at high magnification, was seen to consist of discrete immunoreactive beads. In contrast with the scarcity of labeled cell somata, a heavy band of homogeneous neuropil labeling delineated the whole width of sublayer Ia of the AOL (Fig. 1E), and abruptly decreased at the border with sublayer Ib. At high magnification this labeling appeared as a homogeneous, amorphous impregnation that we interpret as extracellular Reelin. In addition, rows of bead-like labeled particles delineated some neurites. Neuropil immunostaining was virtually absent in layers II and III.

The pyriform cortex (Pir) contained ReIn-ir neuronal somata in all its layers, but most prominently in layer II (Fig. 2A and B). Layer II ReIn-ir cells were pyramidal or bitufted, and the labeling often delineated their proximal dendrites and axons. Thionin counterstain (not illustrated) showed that ReIn-ir somata constituted the superficial cellular rows of layer II, whereas most somata in the deep parts of the layer were unlabeled. There was, in addition, a progressive shift of the labeling in layer II along the rostro-caudal extent of Pir: ReIn-ir cells were scant and very superficial in rostral Pir, near the transition to AOL, but were progressively more numerous and tightly packed in the intermediate and caudal levels of Pir, where they constituted the full thickness of layer II. In addition, scattered fusiform or multipolar cells in Pir layer III were ReIn-ir.

LOT axons running subpially in Pir showed clear bead-like labeling at high magnification; nevertheless, as already noted in AOL, this labeling appeared relatively weak at low magnification. In addition, as in the anterior olfactory nucleus, the neuropil in the outer zone of Pir layer I (sublayer Ia) was strikingly ReIn-ir (Fig. 2A and B). The width and sharpness of the inner border of this band of heavily labeled neuropil decreased caudally in Pir (compare Fig. 2A and B with Fig. 2D). In addition, sublayer Ib, and layers II and III of Pir showed fainter but evident immunolabeling of their neuropil in comparison with the labeling in the amygdala (Fig. 2D).

TABLE 2. Localization and relative proportion of Reelin-immunoreactive neuronal somata and neuropil in rat diencephalic and brainstem regions

	Neuronal somata	Neuropil / axons
Hypothalamus and prethalamic structures		
Zona incerta + Fields of Forel	○○	+
Reticular thalamic nucleus	—	—
Ventral lateral geniculate nucleus	○○○	
Entopeduncular nucleus	○○	+
Subthalamic nucleus	—	—
Hypothalamus		
Paraventricular nucleus	●○○	++
Mammillary bodies	—	—
Other hypothalamic nuclei and areas	○○	+
Dorsal thalamus and epithalamus		
Anterodorsal thalamic nucleus	○○○	+
Dorsal lateral geniculate, lateral posterior, intralaminar nuclei	○○	++
Other dorsal thalamus nuclei.	—	—
Habenular nuclei + Fasciculus retroflexus	○	++
Pretectum and mesencephalon		
Pretectal nuclei		
Olivary pretectal nucleus	●○○	++
Other pretectal nuclei	○○○	+
Superior colliculus		
Zonale and superficial gray strata	●○○	+++
Other strata	○○	+
Inferior colliculus		
Dorsal cortex	○○	++
Other subdivisions	○	+
Periaqueductal gray matter	○	+
Terminal nuclei of the accessory optic system	○○	+++
Substantia nigra		
Pars compacta,	○	+
Pars reticulata	—	—
Ventral tegmental area	○	—
Raphe nuclei	○○	+
Interpeduncular nucleus	○	+++
Pons, cerebellum, medulla oblongata		
Raphe nuclei	○○	+
Reticular nuclei	○	—
Principal, oral and interpolar spinal trigeminal nuclei	—	—
Caudal spinal trigeminal nucleus	○○	+
Basilar pons nuclei	○	+
Superior olivary complex	—	+
Parabrachial complex	—	—
Cochlear nuclei		
Granule cell layer	○○○	+
Other cochlear nuclei	—	+
Vestibular nuclei	—	—
Cranial motor nuclei	—	—
Cerebellar cortex		
Molecular layer	○	+++
Purkinje cell layer	—	—
Granular layer	○○○	—
White matter	—	—
Deep cerebellar nuclei	○	—
Inferior olivary nucleus	—	+
Ventrolateralreticular nucleus	○○	—
Cuneate and gracilis nuclear complex	○	—

Graphic conventions as in Table 1.

In addition to AOL and Pir, all the remaining basal telencephalic target fields of mitral cell axons (LOT axons), namely the olfactory tuberculum (TuO), the nucleus of the lateral olfactory tract, and the cortical (ACo) and medial (AMe) nuclei of the amygdala, contained a band of heavy neuropil labeling in the outer part of their subpial

(molecular) layer. Some of these nuclei contained several ReIn-ir cell somata in their deep tiers; however, an important observation is that the TuO lacked ReIn-ir cell somata (Fig. 2A).

Reelin immunoreactivity in septum, amygdala and basal ganglia

The different septal nuclei contained numerous ReIn-ir cells (Fig. 2C), but staining intensity varied markedly among the nuclei. Numerous immunoreactive cell somata were present in the diagonal band nuclei (Fig. 2C and D) and in the preoptic areas. The anterior area and the basal and lateral nuclei of the amygdala contained scattered ReIn-ir neurons (Fig. 2A and D). The central amygdaloid nucleus, by contrast, contained no labeled neuronal somata. It is noteworthy that the neuropil of the amygdala nuclei showed a consistently lower level of neuropil staining than the adjacent cerebral cortex (Fig. 2D). As noted above, neuropil labeling was heavy in the superficial part of the molecular layer of the cortical and medial amygdaloid nuclei.

Large numbers of striatal neurons were weakly ReIn-ir (Fig. 3). We did not attempt to investigate age-related changes; however, it is of note that this striatal immunostaining was always stronger in young adult rats (2–5 months of age), but much fainter and less widespread in older animals. The labeled neurons were multipolar and ranged from 14 to 20 μm in longer diameter, suggesting that they may mainly be mid-sized spiny neurons. At high magnification, their labeling was seen to consist of very small discrete particles that were distributed in the perikaryon and dendritic shafts (Fig. 3E). The ReIn-ir cells showed an uneven, patchy distribution throughout the caudate-putamen (CPu). They were more abundant in the rostral and intermediate levels of CPu, particularly in its lateral and ventral portions, as well as in the medial region of the caudal CPu. By contrast, they were scarce in the dorsomedial part of the rostral and intermediate CPu, and in the lateral part of the caudal CPu. Labeled neurons were absent from the nucleus accumbens. Groups of more intensely ReIn-ir neurons delineated patch-like domains within the CPu, in a pattern reminiscent of the striosomal compartment of rat striatum. To examine the possibility that the patches of heavily ReIn-ir neurons actually corresponded to striosomes, we compared Reelin-labeled sections with adjacent sections immunostained for the μ -opioid receptor, a specific marker for the striosomal compartment (Fig. 3A and A'). This confirmed that the patches of strongly ReIn-ir neurons largely coincide with the striosomes. However, the experiment also showed that many other ReIn-ir cells are located in the matrix compartment throughout the CPu, particularly in the ventrolateral portions of the nucleus. Western blot analysis of striatal tissue samples provided additional evidence that the immunolabeling observed in the striatal neurons is specific for Reelin protein (see Supplementary material, Fig. S2), and indicated that the prevalent Reelin product in the striatum is the 180-kDa peptide.

Except for a few occasional multipolar cells, the dorsal and ventral pallida were unlabeled (Fig. 2A). Numerous fibers of the stria terminalis were weakly ReIn-ir. In addition, weakly ReIn-ir neurons were present in the nucleus of the stria terminalis.

Reelin immunoreactivity in the isocortex and the hippocampal formation

Neuronal somata showing different intensities of immunostaining were present in all layers of the isocortex. Scattered ReIn-ir cells were also present in the subgriseal lamina (layer VII) and in the cortical white matter. The prevalence of ReIn-ir cells in the various cortical layers displayed slight differences between the cytoarchitectonic fields

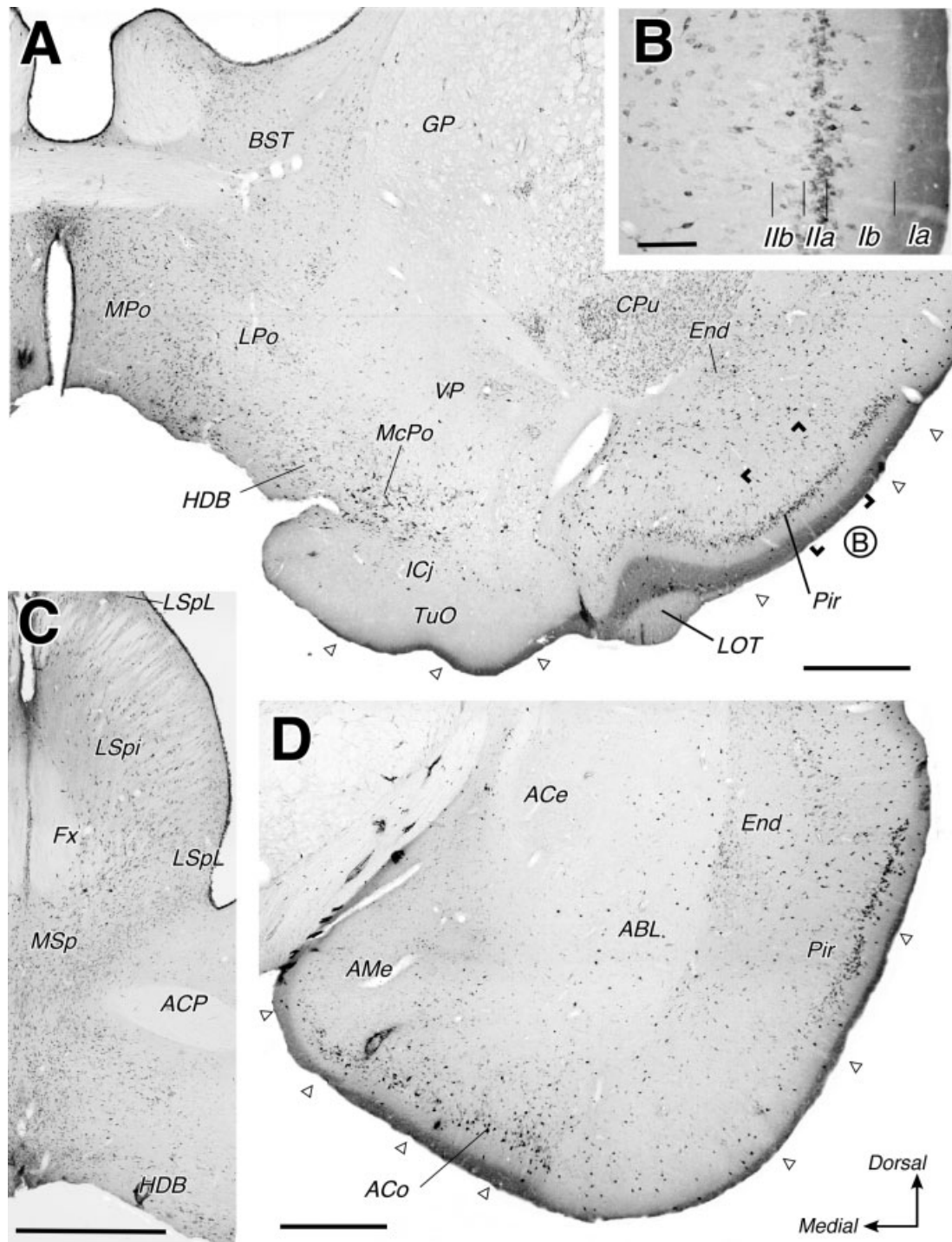


FIG. 2. Reelin-like immunolabeling in basal forebrain and pyriform lobe. (A, C and D) Panoramic views of coronal sections at three different levels showing the ReIn-ir cells and neuropil. In A and D, note the band of heavy neuropil labeling in the superficial layer of the pyriform cortex (Pir), the olfactory tubercle (TuO) and the cortical (ACo) and medial (AMe) amygdaloid nuclei; labeling matches the known terminal distribution of the mitral cell axons. The sublaminar distribution of this labeling in Pir can be better appreciated in the higher-magnification view in B. Note in D that, in addition, there is faint neuropil immunolabeling throughout the deeper layers of the Ppir, ACo, AMe and the endopyriform nucleus (End), whereas such labeling is much weaker or absent from the basolateral (ABL) and central (ACe) amygdaloid nuclei. In addition, numerous neuronal somata are immunoreactive in most of these structures as well as in the preoptic areas (PoA), substantia innominata (SI) and medial septum (MSp). The olfactory tubercle, however, does not contain virtually any labeled cell somata. (B) Detail of the immunolabeling in the superficial layers of Pir. The band of heavily labeled pyramidal cells in layer II is limited to the superficial part of the layer (sublayer IIa), while the deeper pyramids of this layer are unlabeled (IIb) Compare with Fig. 1D. For other abbreviations, see List. Scale bars, 500 μ m (A, C and D); 100 μ m (B).

(Fig. 4A). A weak level of neuropil labeling was apparent throughout the isocortical gray matter; this labeling became markedly heavier in the outer part of layer I, near the pia.

Sublayer Ia of the isocortex contained only heavily staining neurons (soma diameter of 15–30 μ m) with a multipolar shape, but without a preferred dendrite orientation (Fig. 4B). The somata of a few of these

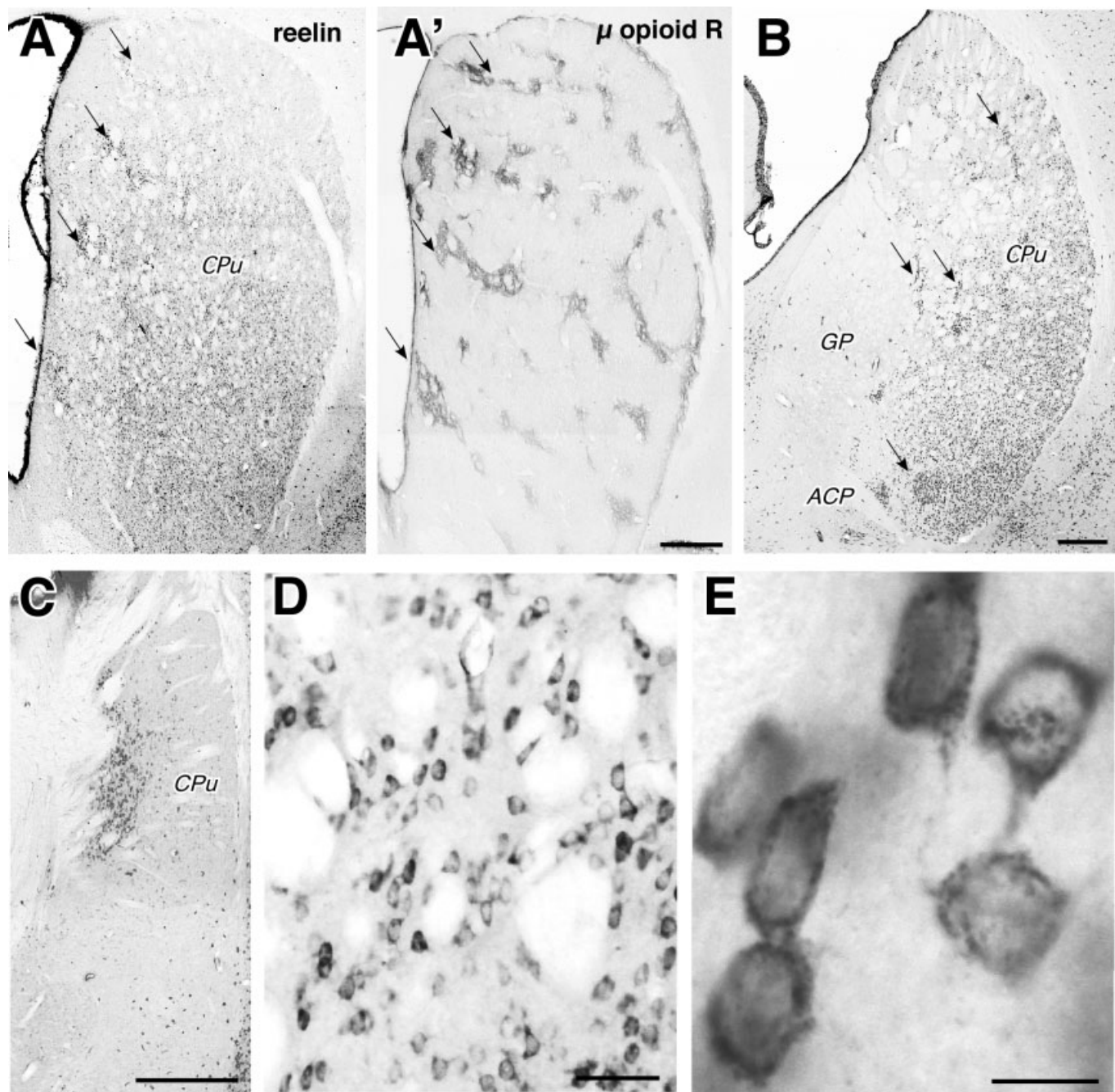


FIG. 3. Reelin-like immunolabeling in the striatum. (A) Panoramic view of Reelin-immunostained coronal section of the caudate-putamen (CPu) from the rostral part of the nucleus (bregma + 1 mm). Note the large numbers of ReIn-ir cell somata in the lateral and ventral CPu and the discrete groups of labeled cells in the dorsal part of the nucleus (arrows). (A') A section adjacent to that shown in A is immunostained against the μ opioid receptor to delineate the striosomal compartment of CPu. Note the close correspondence between striosomes (arrows) and the Reelin-rich cell groups shown in A. (B and C) Reelin-immunostained coronal sections taken from middle (B, bregma -0.90 mm) or caudal (C, bregma -3.30 mm) CPu levels. Note the uneven distribution of ReIn-ir cells. Groups of heavily staining neurons similar to those shown in A are present throughout CPu. In C, note that ReIn-ir cells are largely limited to a medial portion of caudal CPu. (D) Medium-magnification view of the CPU labeling. Note that most CPU cells are labeled but staining intensity varies markedly between them. (E) High-magnification view of labeled neuronal somata. Note the uneven distribution of the immunoprecipitate in the cytoplasm. For other abbreviations, see list. Scale bars, 500 μ m (A–C); 50 μ m (D); 10 μ m (E).

neurons were located at the surface of the cortex, just below the pia. Sublayer Ib as well as layers I–VIII contained several types of weakly stained small (soma diameter 7–15 μ m) cells, and darkly stained medium-sized (15–30 μ m) interneuron-like cells of either bipolar or multipolar shape (Fig. 4D).

In addition, numerous layer V pyramidal neurons in all of the isocortical areas were ReIn-ir (Fig. 4A). Overall, most of these

pyramidal cells displayed moderate to weak labeling. In areas with a well-developed layer V, such as the motor and somatic sensory cortex, the most intensely labeled pyramidal cells were preferentially located in sublayer Va. Weakly ReIn-ir pyramidal cell somata were visible in layer III of some dorsomedial areas such as the cingulate cortex (Fig. 4A). The appearance of the labeling at high-magnification in these pyramidal cell somata was identical to that of many other ReIn-ir

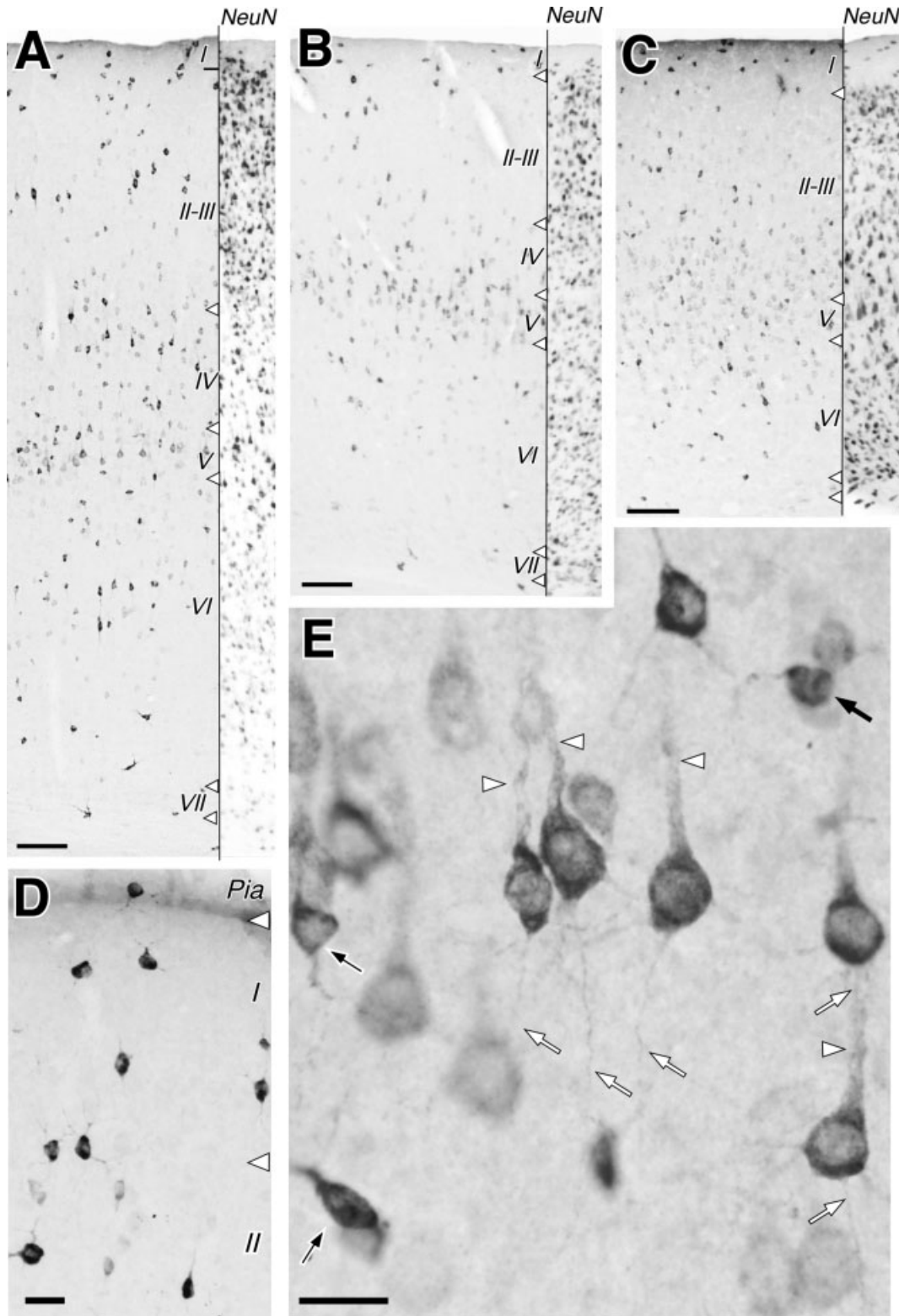
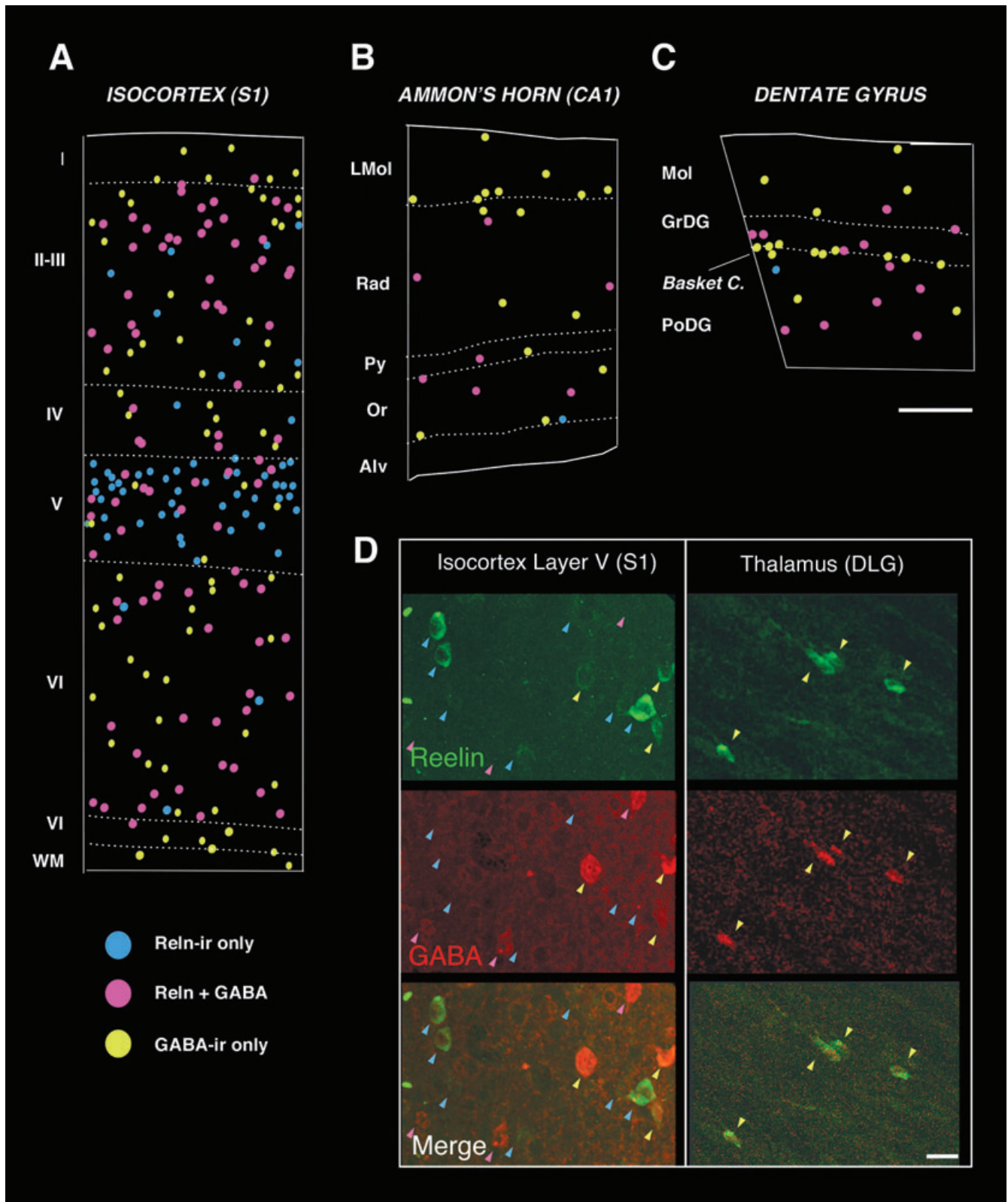


FIG. 4. Reelin-like immunolabeling in the cerebral cortex. (A–C) Coronal section samples of primary somatosensory area (A), primary visual area (B) and cingulate cortex (C). For cytoarchitectonic comparison, a parallel section immunostained for NeuN is aligned at the right side of each panel. Note that ReIn-ir somata are present in all cortical layers, as well in the subcortical white matter, but fairly more numerous in layer V. A faint neuropil labeling is present throughout the cortical gray matter, and is most evident in the outer part of layer I, near the pial surface. This labeling is not a border artifact of the DAB immunostaining; see, for comparison, the NeuN-immunostained samples. The layer I neuropil staining is particularly heavy in the cingulate cortex. (D) Detail of the labeling in the upper layers of the somatosensory cortex. Note the multipolar or fusiform shape and the heavy labeling of the neurons labeled in this layer. (E) High-magnification view of layer V neurons in the somatosensory cortex. Numerous large pyramidal neurons contain intracytoplasmic immunolabeling that delineates the cell nucleus and extends into the proximal dendrites (arrowheads) as well as into the axon (white arrows). Some layer V interneurons are also ReIn-ir (black arrows). For abbreviations, see List. Scale bars, 250 μm (A–C); D and 20 μm (E).

neurons throughout the brain: uneven or lump-like, and always absent from the nucleus, indicating its intracellular location (Fig. 4E). Some of these elongated lumps extended for up to 50 μm into the stalk of the apical dendrite. Overall, this pattern is consistent with the light-microscopic appearance of labeled endoplasmic reticulum and Golgi

cisterns of cortical pyramidal cells (De Camilli *et al.*, 1986; Martínez-Cerdeño *et al.*, 2002).

The size and dendritic morphology of the layer V neurons made it quite evident that most of them were pyramidal neurons. Nevertheless, because the immunolabeling did not completely reveal the dendritic



tree of these cells, we double-stained for Reelin and GABA on single sections to substantiate further that the Reelin-ir pyramidal cells were not GABAergic interneurons with an ambiguously shaped soma. Analysis of this material (Figs 5A and D, and 6A and D) revealed that whereas about 90% of Reelin+ cells in all other cortical layers co-localized GABA, only about 20% of the Reelin+ cells in layer V co-localized GABA. These observations confirm that numerous non-GABAergic pyramidal cells in cortical layer V contain intracellular Reelin. In addition, the double-labeling analysis revealed that Reelin and GABA colocalization is virtually complete in layers I and VII, but not in other layers.

Layer I of the entorhinal areas contained markedly fewer Reelin-ir cells than layer I of the isocortical or subicular fields. Comparison with parallel NeuN-immunostained sections (not shown) seems to indicate that this difference simply reflected the much lower overall number of neurons in layer I of the entorhinal cortex as compared with the isocortex. In the lateral entorhinal area (LEA), large numbers of layer II pyramidal cells were heavily Reelin-ir (Fig. 7A–C). Thionin counterstaining revealed that, in fact, virtually all the layer II cells were Reelin-ir. The pyramidal cells of layer III were labeled as well, although less heavily (Fig. 7A and B). In the deep strata of LEA, immunolabeled neurons were less numerous, whereas more scattered neurons are present in the deep strata of LEA. In addition, all the LEA layers contained other labeled neurons with a fusiform or multipolar shape. Neuropil labeling was present in the superficial part of LEA layer I, a terminal field for LOT axons (Price, 1973). In contrast to LEA, pyramidal cells in layer II of the medial entorhinal area (MEA) showed uniformly low labeling in their somata (Fig. 7A).

The axons of the entorhinal layer II cells showed the same type of bead-like labeling described above for mitral cell axons. Despite the relatively weak and discontinuous nature of this labeling, and the fact that we did not use metal enhancement of the DAB staining, it was possible to follow these axons, at 1000 \times , far into the white matter as they converged into the angular bundle and entered the subiculum (Fig. 7C–E). Remarkably, the known terminal field of these axons in the hippocampus [the superficial part or the molecular layer of the dentate gyrus (DG) and the stratum lacunosum-moleculare of Ammon's horn (CA); Amaral & Witter, 1994] was delineated by a band of heavy neuropil immunolabeling (Fig. 7F). It is also of note that the axons of neurons in layer III of LEA also project to the stratum lacunosum-moleculare of the CA (Deller *et al.*, 1996). Taken together, the above observations indicate that the whole entorhino-hippocampal

pathway (cells of origin, axons and terminal neuropil) is heavily Reelin-ir in adult rodents.

Most pyramidal cells in the pyramidal strata of the pre- and parasubiculum were Reelin-ir. In addition, some cells with an interneuronal shape were located in layer I, and less frequently, also in the pyramidal strata of these areas (Fig. 7A). In the subiculum proper, pyramidal cells were not labeled.

Pyramidal cells in the Ammon's horn fields of the hippocampus (CA1–CA3) were unlabeled. These fields contained, however, several populations of heavily immunoreactive multipolar or bipolar interneuron populations usually displaying labeling in their proximal dendrites (Fig. 7F–H). The laminar distribution of CA1–CA3 Reelin-ir cells was highly heterogeneous. (Fig. 7F and G). Numerous cells were labeled along the border between the strata oriens and lacunosum-moleculare as well as in the deep part of the stratum oriens. Additional cells were scattered in the radiatum and pyramidal strata. Double-immunostaining for Reelin and GABA revealed that virtually all cells in the stratum lacunosum-moleculare co-localize both markers (Figs 5B and E, and 6B).

In the DG, several populations of interneurons were immunostained; however, there was no labeling in granule cells (Fig. 7F and H). A large population of basket cells were heavily stained. Co-localization of GABA and Reelin was virtually complete in the basket cells (Figs 5C and F, and 6C). The DG molecular layer contained relatively few labeled neurons. As mentioned above, a band of heavy neuropil labeling covered the outer part of the DG molecular layer and the stratum lacunosum-moleculare of CA (Fig. 7F). The high-magnification appearance of this neuropil labeling again revealed an amorphous staining and numerous rows of fine bead-like particles that we interpret as labeled neurites.

Reelin immunoreactivity in diencephalic structures

In the dorsal thalamus, Reelin-ir cell somata were limited to a few nuclei. The most prevalent labeling was observed in the anterodorsal and paraventricular nuclei (Fig. 8A and D). Numerous weakly immunolabeled cells were also present in the anterior intralaminar nuclei such as the central medial, paracentral and central lateral. In addition, a conspicuous population of Reelin-ir neurons was scattered throughout the dorsal lateral geniculate (DLG) and lateral posterior (LP) nuclei (Fig. 8C). These DLG and LP cells were mainly bipolar, and their smooth dendrites were often labeled for several

FIG. 5. Laminar distribution and co-localization analysis of Reelin and GABA immunoreactivity in neuronal cell somata of the isocortex, hippocampal formation and thalamus. (A) Laminar distribution of neurons immunoreactive for Reelin (black bars) or GABA (gray bars) in the isocortex (parietal cortex area S1). Bars represent, for each marker, the fraction of the total of immunoreactive cells present in each layer. Total numbers of cells immunoreactive for each marker are shown below the chart. Note that laminar distribution of Reelin-immunoreactive (Reelin-ir) cells is uneven: layer V, despite being relatively thin, contains a large fraction of Reelin-ir cells. By contrast, GABA-immunoreactive (GABA-ir) cells are homogeneously distributed across layers, as the apparent differences between layers simply reflect the layer thickness. (B) Laminar distribution of immunostained neurons in Ammon's horn sectors CA1 and CA3. Graphic conventions as in A. For cell layer abbreviations, see List. (C) Laminar distribution of immunostained neurons in the dentate gyrus. Graphic conventions as in A. Because of their characteristic position and prominent immunolabeling, the basket cells are singled out here as a distinct cell layer ('Basket C.'). For other cell layer abbreviations, see List. (D) Co-localization analysis of Reelin and GABA immunolabeling in isocortical cells. In parallel bars for each marker, the chart displays co-localization ratio (as a percentage) over a possible maximum of 100%. Data are provided both for the cortex as a whole ('Global', top row) and for each cortical layer. Black bars represent the percentage of Reelin-ir cells co-localizing GABA-immunolabeling. Gray bars represent the percentage ratio of GABA-ir cells co-localizing Reelin immunolabeling. Note that, for each row, the blank space extending up to the right margin of the chart (100%) stands for the ratio of cells immunoreactive for the corresponding marker that do not co-localize the other marker. Note that only about 20% Reelin-ir cells in layer V co-localize GABA. By contrast, the ratio of GABA cells co-localizing Reelin in this layer is the same (around 45%) as that in layers II–III, IV, and VI. Together with data in A, these results show that layer V contains a large, layer-specific population of non-GABAergic cells that are Reelin-ir. As a significant internal control, Reelin and GABA co-localization is virtually complete in layers such as layer I ('I') or the subgriseal layer and interstitial white matter cells ('VII-WM'). (E) Co-localization analysis of Reelin and GABA immunolabeling in Ammon's horn sectors C1 and CA3. Graphic conventions as in D. For abbreviations, see List. Reelin-ir and GABA-ir cells are the same cell population; by contrast, the other hippocampal strata contain significant populations of GABA-ir neurons that do not contain Reelin. (F) Co-localization analysis of Reelin and GABA immunolabeling in the dentate gyrus. Graphic conventions as in D. (G) Co-localization analysis of Reelin and GABA immunolabeling in several thalamic nuclei. Co-localization ratios in each nucleus are displayed separately. Because differences in co-localization ratios are extreme, and the distributions of Reelin-ir and GABA-ir cells in the rat thalamus are highly anisotropic, in this case there is no point in pooling together data from different nuclei in a global ratio for the thalamus as a whole. Other conventions as in D. For abbreviations, see List.

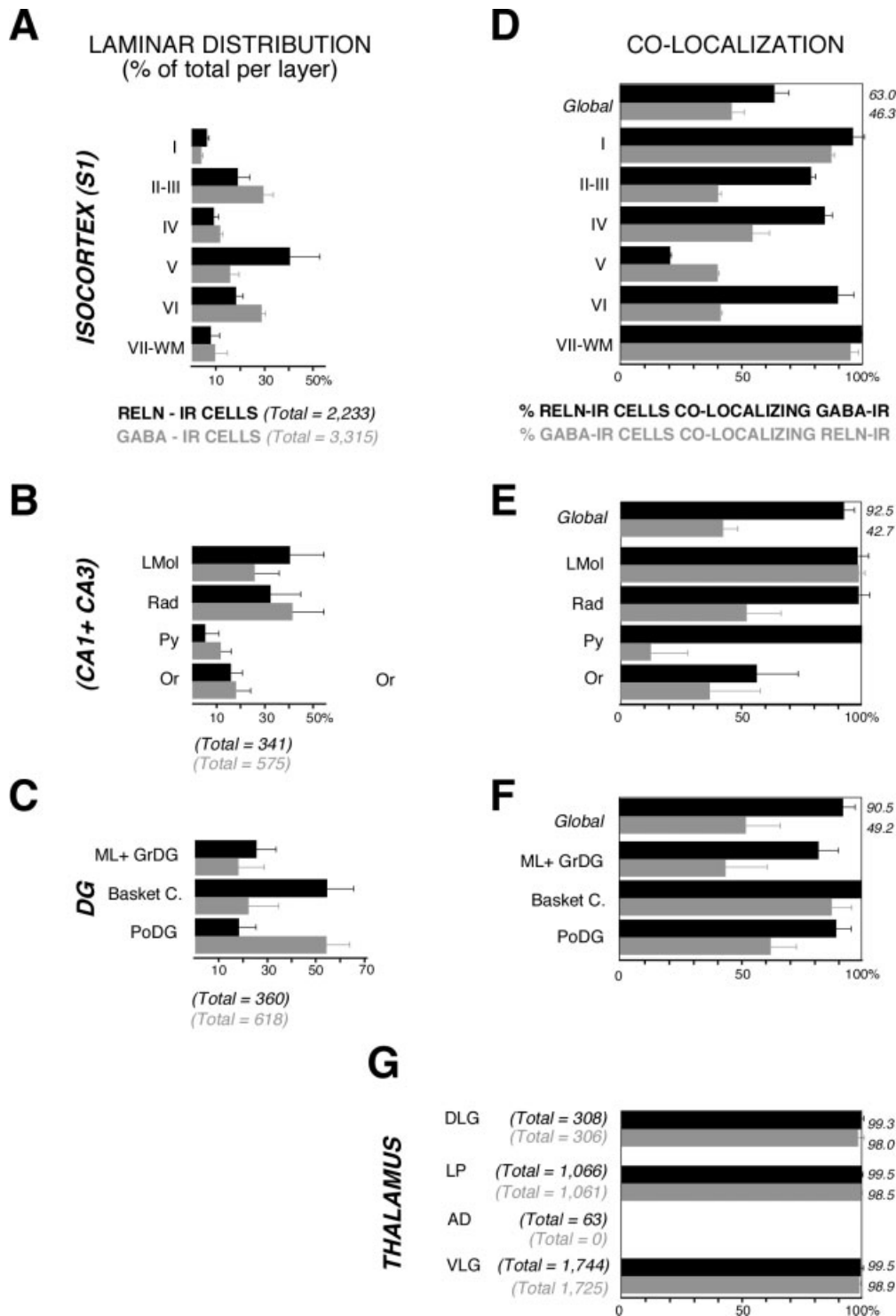


FIG. 6. Reelin and GABA co-localization in cerebral cortex and thalamus. (A–C) Plots of cells immunolabeled for both Reelin and GABA (yellow dots), cells immunolabeled only for Reelin (blue dots) and cells labeled only for GABA (pink dots) in representative samples of the isocortex (A), the CA1 sector of the hippocampus (B) and the suprapyramidal blade of the dentate gyrus (C). Note in A that the population of Reln-ir cells that do not contain GABA is preferentially concentrated in layer V. Note also the high prevalence of neurons co-localizing both markers in cells in the subpial layer of the three fields. (D) Four-micrometer-thick confocal optical section samples of layer V of the parietal isocortex (left column) and dorsal lateral geniculate thalamic nucleus (right column) are shown. Comparison of these images obtained through each excitation/reveals numerous cells staining either for Reelin (blue arrowheads) or GABA (pink arrowheads) in the sample from layer V of the isocortex. Yellow arrowheads indicate cells co-localizing both markers. The pyramidal morphology of some of the Reelin-only cells is evident even in these thin optical sections. Note that all cells labeled in the dorsal lateral geniculate nucleus co-localize both GABA and Reelin. Scale bar, 20 μ m.

hundred micrometers (Fig. 8E). They were markedly smaller ($8.5 \pm 1.5 \mu$ m minimum soma diameter) than the general population of the neurons in these two nuclei as revealed by Thionin or NeuN

staining ($12 \pm 1.3 \mu$ m minimum soma diameter; compare Fig. 8D and E). The Western blot analysis of LP tissue samples provided additional evidence that the immunolabeling observed in the

population of thalamic neurons is specific for Reelin protein. As in other brain regions, the most abundant Reelin peptide detected in the thalamus is the 180-kDa fragment (see Supplementary material, Fig. S2).

These observations raised the possibility that the LP and LGD cells were the intrinsic GABAergic interneurons that are known to exist in these nuclei of the rat thalamus (Ohara *et al.*, 1983). To investigate this possibility, we examined thalamic double-immunostained for Reelin and GABA (Figs 5G and 6D). GABA immunoreactivity in the neuronal somata varied widely in intensity, as previously reported (Ohara *et al.*, 1983). The co-localization analysis revealed that virtually all Reelin-ir LGD cells contained GABA. The same was the case for the LP Reelin-ir neurons (Fig. 5G). By contrast, the remaining thalamic nuclei containing Reelin-ir (anterodorsal, paraventricular and anterior intralaminar) contained no GABA cells (Fig. 5G), as previously reported (Ohara *et al.*, 1983); thus, the Reelin-containing cells in these nuclei are projection neurons.

Neuropil labeling was absent throughout the dorsal thalamus, except for a weak but consistent labeling in LGD and LP.

Most cells in the medial habenular nucleus were heavily Reelin-ir (Fig. 8B). A Reelin-ir population was also present in the lateral nuclei, although most of the cells in this nucleus were not labeled. The habenulo-interpeduncular tract displayed faint labeling that, when examined at high magnification, had a punctate appearance similar to that observed in LOT and the angular bundle (Figs 8C and 9B). Interestingly, the neuropil of the interpeduncular nucleus (Fig. 10A), which is a main target of these axons, was heavily Reelin-ir.

Labeled neurons were very numerous in several prethalamal (previously referred to as 'ventral thalamic', see Puelles & Rubenstein, 2003) structures, as well as in some hypothalamic nuclei. The nucleus of the stria medullaris contained a densely packed group of Reelin-ir cells. A population of small, weakly Reelin-ir cells was scattered along the inner border of the external medullary lamina and the ill-defined ventral reuniens nucleus (Fig. 8A and B); by contrast, the adjacent reticular thalamic nucleus was not labeled. Weakly labeled cells were scattered in the dorsal zona incerta, fields of Forel and entopeduncular nucleus. Most cells in the ventral lateral geniculate nucleus were Reelin-ir; interestingly, the cells in its magnocellular subnucleus were much more heavily stained than those in the parvocellular subnucleus or the intergeniculate leaflet (Fig. 8C). Double-labeling for Reelin and GABA (Fig. 5G) revealed that in this nucleus co-localization was virtually total.

The paraventricular hypothalamic nucleus was delineated by heavy immunolabeling of the neurons in its dorsal cap and lateral magnocellular subdivisions (Fig. 8B). Other subnuclei were virtually free of labeled neurons. The posterior hypothalamic-midbrain transition area ('PH' in Fig. 8C) contained a heavily Reelin-ir cell population. The dorsal and lateral hypothalamic areas, however, contained only scattered Reelin-ir neurons, most of which were weakly stained.

The pretectal region showed widespread Reelin immunolabeling, and all its nuclei contained numerous Reelin-ir somata. The labeling in the olivary pretectal nucleus was remarkable: virtually all its neurons were heavily labeled, and its neuropil was heavily immunostained (Fig. 8C and F).

Reelin immunoreactivity in the brainstem and retina

Among the brainstem regions, the mesencephalic tectum and the cerebellar cortex showed heavy and widespread Reelin immunolabeling. By contrast, immunoreactivity in the pons and medulla was limited to isolated groups of weakly labeled cells.

Large numbers of Reelin-ir cells were visible in the superior colliculus. The most numerous and heavily labeled cells were located in the superficial strata of the superior colliculus (Fig. 9B and C). In addition, the zonal and superficial gray strata showed heavy neuropil immunolabeling. At high magnification, this labeling consisted of an amorphous staining and numerous neurites made visible by immunostained puncta. The labeled neuropil distribution matched the known terminal pattern of retinotectal axons (Sefton & Dreher, 1994; Sakakibara *et al.*, 2003). Moreover, the accessory optic tract nuclei neurons and their neuropil were Reelin-ir (Fig. 9B). These observations prompted us to examine Reelin immunolabeling in the adult rat retina (Fig. 9D). A substantial population of retinal ganglion cell somata, their proximal dendrites and their initial axon segments were Reelin-ir. In addition, weak labeling was present in some cell somata in the inner nuclear layer. A prominent band of heavy neuropil immunolabeling delineated the IPL. The remaining retinal layers were free of labeling.

The inferior colliculus contained numerous labeled neurons (Fig. 10A–C) that were most abundantly and heavily stained in the collicular cortex. The periaqueductal gray matter contained Reelin-ir cells that were most abundant in its dorsal portions. The large neurons of the nearby nucleus of Darkewisch were heavily Reelin-ir as well. Numerous Reelin-ir neurons were present in the raphe nuclei (Figs 9B and 10A, D and E). The periaqueductal gray matter contained Reelin-ir cells that were most abundant in its dorsal portions. The large neurons of the nearby nucleus of Darkewisch were heavily Reelin-ir as well. Numerous Reelin-ir neurons were present in the raphe nuclei (Figs 9B and 10A, D and E). Some lateral tegmental nuclei related to the auditory pathways, such as the nuclei of the lateral lemniscus and the nucleus of the brachium of the inferior colliculus (Fig. 9A), contained weakly Reelin-ir cells. The remaining mesencephalic tegmentum areas were unlabeled or contained only occasional stained cells.

The main nuclei of the trigeminal complex and other cranial motor and sensory nuclei lacked immunolabeling. However, the caudal portion of the spinal trigeminal nucleus in the medulla oblongata showed weak but consistent staining of numerous cells in the superficial sublayer of the nucleus, adjacent to the fibers of the spinal trigeminal tract (Fig. 10J and K). In addition, the most conspicuously Reelin-ir cells in the medulla oblongata were those of the ventrolateral reticular nucleus; scattered cells were also present throughout the lateral reticular nucleus and raphe nuclei.

The cerebellar cortex showed heavy neuropil labeling of the molecular layer and dense labeling in the granule cell layer (Fig. 10H and I). Additional weakly labeled somata were present in the molecular layer. The Purkinje cells and the cerebellar white matter were unstained.

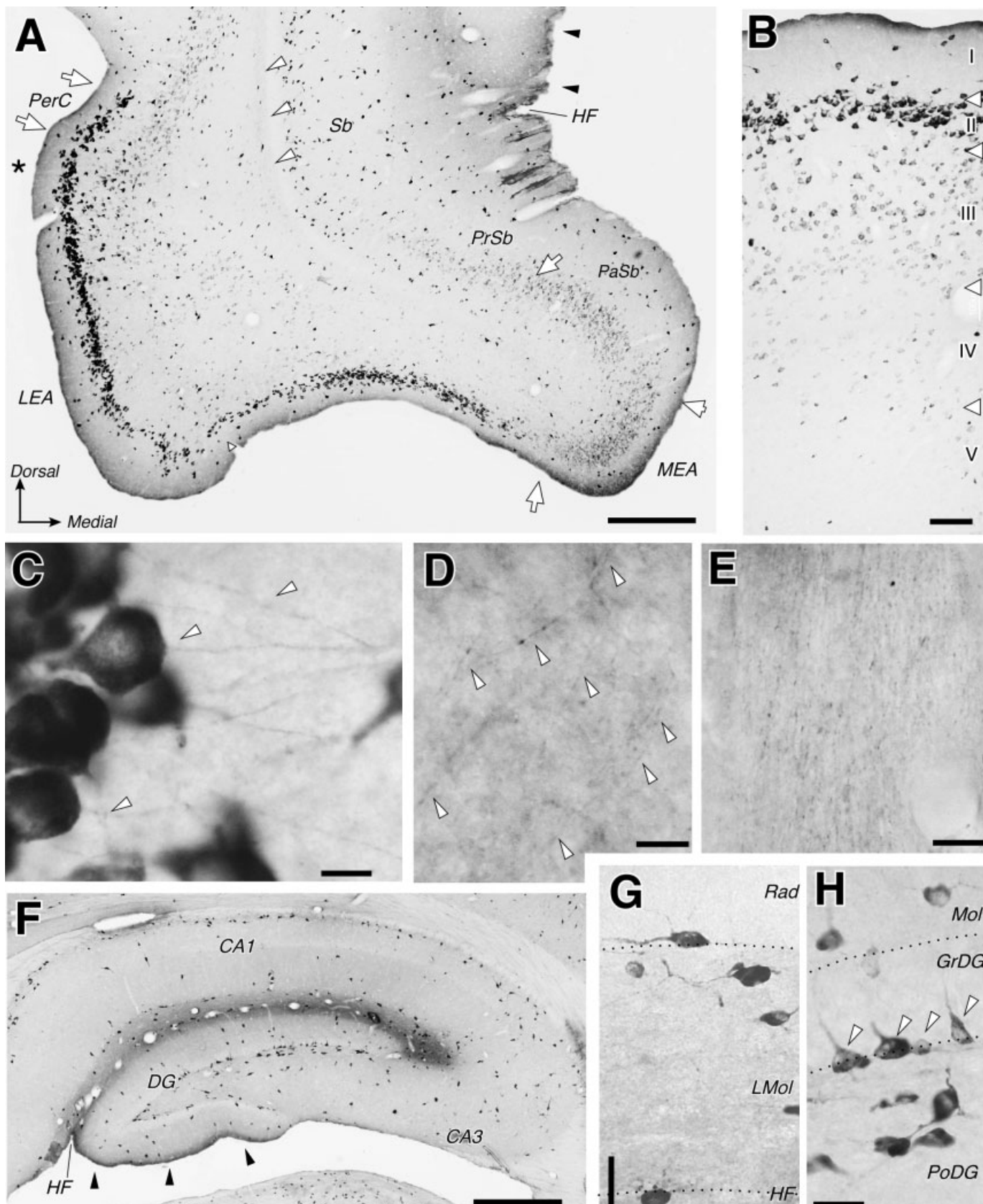
Discussion

We have systematically mapped the localization of Reelin-like immunoreactivity throughout the forebrain and brainstem of the adult rat. Our data reveal that Reelin is preferentially present in neuron populations of the forebrain and the cerebellar cortex, and much scarcer in the pons and medulla. Results are largely consistent with previous mRNA ISH studies in rodents (Ikeda & Terashima, 1997; Alcántara *et al.*, 1998; Pesold *et al.*, 1998; Haas *et al.*, 2000), and confirm and extend the available immunolocalization data (Miyata *et al.*, 1996; Drakew *et al.*, 1998; Pesold *et al.*, 1998; Nishikawa *et al.*, 1999; Pérez-García *et al.*, 2001; Martínez-Cerdeño & Clascá, 2002). In addition, we

report the presence of other Reelin-containing cells and neuropil areas, mostly in brain structures not specifically examined in the previous studies.

Specificity and interpretation of the immunolabeling

Labeling included cell somata, dendrites, axons and extracellular neuropil staining, all of which displayed a broad range of staining



intensity. This pattern is consistent with the expectation that, unlike Reelin mRNA, which remains in the perikaryon of synthesizing cells (D'Arcangelo *et al.*, 1995; Schiffmann *et al.*, 1997; Alcántara *et al.*, 1998; Haas *et al.*, 2000), the Reelin protein can be found: (1) in the endoplasmic reticulum and Golgi complex of synthesizing neurons (Pappas *et al.*, 2001; Martínez-Cerdeño *et al.*, 2002); (2) in membrane-bound vesicles within axons as it is transported for secretion (Derer *et al.*, 2001; Martínez-Cerdeño *et al.*, 2002, 2003; Pappas *et al.*, 2003); (3) in the extracellular matrix and cell membranes of synaptic neuropils after secretion (D'Arcangelo *et al.*, 1997; Pappas *et al.*, 2001; Dong *et al.*, 2003); (4) within re-internalization vesicles after binding to receptors in target cells (D'Arcangelo *et al.*, 1999; Morimura *et al.*, 2005); or even (5) diffusing in the intercellular space, before eventually reaching the cerebrospinal fluid (Saez-Valero *et al.*, 2003; Ignatova *et al.*, 2004).

Given such potential variety, we took pains to ensure the specificity of our staining through an exhaustive set of immunolabeling controls (Saper & Sawchenko, 2003; see Methods and Supplementary Material). The coincident results from all these controls firmly indicate that the observed labeling is specific for Reelin.

It must be kept in mind that Reelin is a very large (~420 kDa) protein with functionally diverse domains, and that it may be cleaved after secretion. The monoclonal antibodies used here recognize only the N-terminal region of Reelin. Specifically, antibody CR-50 binds amino acid residues 246–371, while antibody 142 binds residues 164–189, and antibody G10 binds residues 199–245 (D'Arcangelo *et al.*, 1997; De Bergeyck *et al.*, 1998). This N-terminal region is present in the full-length protein as well as in some of the cleaved fragments but not in others (Lambert de Rouvroit *et al.*, 1999; Jossin, 2004). Thus, immunolabeling in our material may correspond to both full-length Reelin, and any of the cleaved fragments that contain the N-terminal region, but not to the fragments, some of which may still mediate signaling, that lack this region (Jossin, 2004). The N-terminal region allows the homodimerization of secreted Reelin (Utsonomiya-Tate *et al.*, 2000; Strasser *et al.*, 2004), a process which seems to be crucial for the co-operative interactions at the cell membrane (such as clustering and/or internalization of multiple receptors) and which seems to mediate some Reelin effects *in vivo* (D'Arcangelo *et al.*, 1999; Andersen *et al.*, 2003; Sanada *et al.*, 2004; Strasser *et al.*, 2004; Morimura *et al.*, 2005). Antibody CR-50 prevents dimerization and blocks Reelin function *in vitro* and *in vivo* (Ogawa *et al.*, 1995; Del Rio *et al.*, 1997; Nakajima *et al.*, 1997; Kubo *et al.*, 2002; Zhao *et al.*, 2004). In addition, the N-terminal region is the one that binds integrin $\alpha 3 \beta 1$ receptors (Dulabon *et al.*, 2000; Schmid *et al.*, 2005), and this binding may be important for a possible Reelin-mediated local regulation of cell adhesive properties at perisynaptic sites (Rodríguez *et al.*, 2000; Dong *et al.*, 2003; Sanada *et al.*, 2004; Schmid *et al.*, 2005).

Resolving the precise subcellular localization of the immunolabeling requires electron microscopy. However, neuronal somata labeling in Reelin-ir cells strongly resembles the light-microscope appearance of the endoplasmic reticulum and Golgi complex (De Camilli *et al.*, 1986). The presence of Reelin in these cell organelles of the constitutive secretory pathway has been demonstrated by electron-microscopic studies in adult mouse (Pappas *et al.*, 2001) and macaque neurons (Martínez-Cerdeño *et al.*, 2002). Moreover, most of the neuron populations with intracellular labeling match those reported to contain Reelin mRNA in adult rodents (Alcántara *et al.*, 1998; Haas *et al.*, 2000). There are some mismatches, such as Reelin-ir striatal and thalamic cells, which have not been reported to contain Reelin mRNA in ISH studies. Because the specificity of our immunolabeling is firmly established, the incongruence may arise from two alternative, but not mutually exclusive, possibilities. First, these cell populations may express Reelin mRNA at levels that are too low to be detected by the ISH assays on thick tissue sections (Femino *et al.*, 1998; Speel *et al.*, 1999). Only negative results using PCR amplification can effectively rule out the presence of low, but biologically significant, numbers of mRNA transcripts, and, because of post-transcriptional regulatory mechanisms, low mRNA levels do not directly imply low protein levels (Gygi *et al.*, 1999; Tian *et al.*, 2004). In addition, the observation that labeling in these cells is morphologically equivalent to that in other cells known to express Reelin mRNA (compare for example Figs 1A, 3E, 4E, 7C, 8D and E, 10C, G and E, or 10I) also suggests Reelin expression in these cells. A second possibility is that the immunolabeling reveals Reelin internalized in membrane-bound vesicles after binding to lipoprotein receptors (D'Arcangelo *et al.*, 1999; Morimura *et al.*, 2005); thus, it would not require Reelin mRNA expression by the labeled cells.

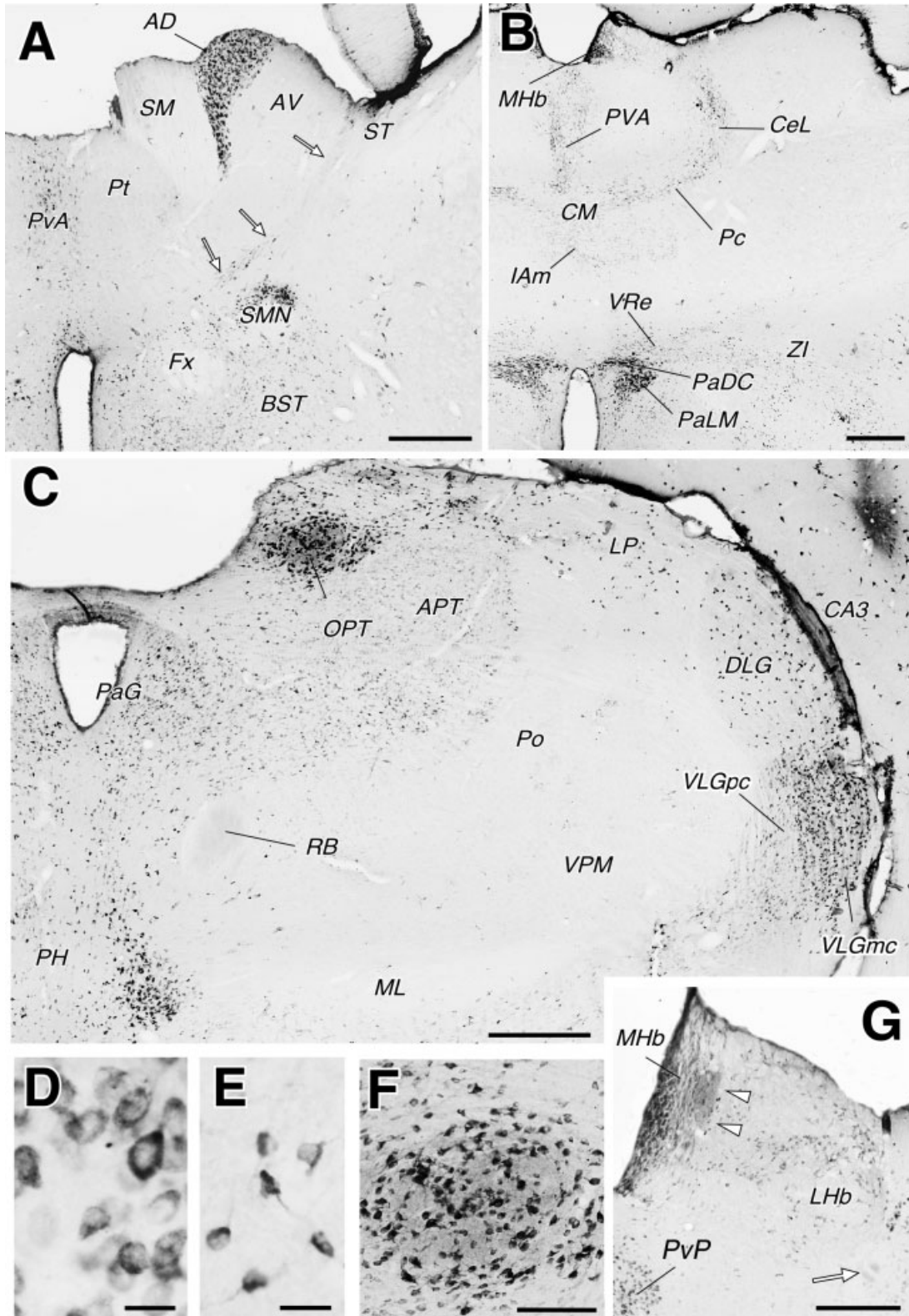
Secreted Reelin is particularly abundant in some spine-rich neuropils

Numerous neuropil areas showed an amorphous/punctate immunolabeling of variable intensity. We could not resolve between the Reelin present within fine axon terminals or distal dendrites and spines, and that which had been secreted to the ECM. Nevertheless, the light-microscope appearance of the immunolabeling largely resembled that noted for other secreted ECM molecules (Dityatev & Schachner, 2003). Interestingly, the heaviest labeling is found in neuropils such as the stratum lacunosum-moleculare of CA1, the pyriform cortex sublayer Ia, the isocortex sublayer Ia or the molecular layer of the cerebellar cortex, all of which are known to contain massive concentrations of dendritic spines. This type of neuropil labeling has been reported in the equivalent brain regions in rodents, carnivores and primates, including humans (Miyata *et al.*, 1996;

FIG. 7. Reelin-like immunolabeling in the parahippocampal cortex and hippocampus. (A) Panoramic view of the entorhinal and adjacent areas in a coronal section at approximately bregma -6.30 mm. White arrows indicate area borders. Arrowheads indicate the labeled axons in the angular bundle beneath the subiculum (Sb, detail in E). Note the heterogeneous distribution and staining intensity of Reelin-ir neuron populations in the various fields. Neuropil labeling is visible in layer I of the entorhinal areas (LEA, MEA). (B) Detail of the immunolabeling in the lateral entorhinal cortex (LEA). Note that most of the pyramidal layer II and III cells contain Reelin. (C) High-magnification view of the labeled somata and axons (arrowheads) of layer II LEA projection neurons. (D and E) High-magnification detail of the particulated immunolabeling in putative layer II entorhinal axons running in the deep layers of the lateral entorhinal area (D, arrowheads) and in the angular bundle under the subiculum (E, compare with the arrowheads in A). (F) Panoramic view of labeling in the dorsal hippocampus taken from a coronal section at about coronal bregma level -4.30. Note the heavily Reelin-ir cells in the strata oriens, lacunosum-moleculare and radiatum of Ammon's horn fields (CA1, CA3) and in the dentate gyrus (DG) hilus. In addition to labeled neuronal somata, there is a sharply delineated band of heavy neuropil labeling throughout the stratum lacunosum-moleculare of CA and the superficial third of the DG molecular layer. This neuropil labeling is present in both the suprapyramidal [within the hippocampal fissure (HF), delineated by blood vessels] and infrapyramidal (arrowheads) DG blades. The labeled neuropil matches the known terminal distribution of layer II LEA projection neurons. Similar but fainter labeling can be seen around HF in A. (G) Detail of field CA1. Reelin-ir cell somata are preferentially located near the border between the strata lacunosum-moleculare (LMol) and radiatum (Rad). (H) Detail of labeled cells in DG. Large Reelin-ir interneurons are labeled in the polymorph (PoDG), granular (GrFD) and molecular (Mol) layers of this field; however, there is no labeling in the granular cells. Arrowheads highlight the large basket interneurons labeled along the border of GnFD and PoDG. For other abbreviations, see List. Scale bars, 500 μ m (A and D); 100 μ m (B); 10 μ m (C and E); 25 μ m (G and H).

Drakew *et al.*, 1998; Pesold *et al.*, 1998; Rodríguez *et al.*, 2000; Pérez-García *et al.*, 2001; Martínez-Cerdeño & Clascá, 2002; Martínez-Cerdeño *et al.*, 2002, 2003; Deguchi *et al.*, 2003; Roberts *et al.*, 2005). Electron-microscopic studies have identified secreted Reelin near dendrites and dendritic spines at extrasynaptic sites (Rodríguez *et al.*, 2000; Pappas *et al.*, 2001, 2003). In the adult brain, dendritic spines

are known to be preferential sites for rapid, activity-induced structural changes that correlate with long-lasting changes in synaptic efficacy such as long-term potentiation or depression (Yuste & Bonhoeffer, 2001; Dityatev & Schachner, 2003; Berardi *et al.*, 2004; Oray *et al.*, 2004). Moreover, there is direct evidence for activity-driven spine remodeling in some of the above Reelin-rich neuropils (Geinisman



et al., 1992; Klintsova & Greenough, 1999; Weeks *et al.*, 1999; Yuste & Bonhoeffer, 2001; Oray *et al.*, 2004).

Evidence for Reelin involvement in the modulation of synaptic plasticity has grown rapidly over the past few years (D'Arcangelo, 2005a). Because of its known ability to influence membrane adhesivity and/or cytoskeletal dynamics in embryonic neurons, the finding of Reelin in adult neuropil areas, near dendritic spines, led to the first suggestions that, similarly, it might regulate adult synaptic remodeling (Impagnatiello *et al.*, 1998; Rodríguez *et al.*, 2000; Rice *et al.*, 2001). A reported intrinsic serine-protease activity of Reelin was suggested as a possible mechanism behind this activity (Quattrocchi *et al.*, 2002; Dityatev & Schachner, 2003). Electrophysiological studies in hippocampal slices showing that Reelin signaling through lipoprotein receptors modulated long-term potentiation provided direct evidence for Reelin involvement in synaptic plasticity (Weeber *et al.*, 2002). This effect has recently been shown to depend on Reelin signaling through a spliced variant of the apolipoprotein receptor 2 that directly modulates the NMDAR (Beffert *et al.*, 2005; Chen *et al.*, 2005). NMDAR is a pivotal molecular switch for the induction of long-term, activity-dependent functional and structural synaptic changes. Additionally, Reelin signaling has also been found to regulate the subunit composition of the NMDAR, a finding that now implicates Reelin in the regulation of critical periods for synaptic plasticity during late postnatal development (Sinagra *et al.*, 2005). Our finding of selectively high Reelin concentrations in several dendritic spine-rich neuropils therefore means that Reelin signaling is in place and available to be a significant modulator of activity-induced synaptic changes in these particular adult brain circuits.

Reelin transport and secretion by adult axonal pathways

In the brain, Reelin is axonally secreted only by neurons (D'Arcangelo *et al.*, 1997; Alcántara *et al.*, 1998; Derer *et al.*, 2001; Pappas *et al.*, 2003); thus, in any ECM, Reelin sources can be the local neurons and/or the terminals of an afferent Reelin-synthesizing pathway.

Most of the Reelin-immunoreactive (Reelin-ir) neuropils reported in this study contain at least some Reelin-expressing neurons, which are an obvious source for the observed ECM Reelin. Interestingly, however, our data also suggest that an extrinsic afferent pathway may be a Reelin source in some of these neuropils. This possibility is particularly clear for the mitral cell projection to olfactory areas of the basal forebrain. Adult mitral cells express high Reelin mRNA levels (Alcántara *et al.*, 1998), their axons (LOT) contain Reelin-ir particles (Pappas *et al.*, 2003; present results), and their terminal fields in sublayer Ia of the molecular layer of the olfactory areas (Price, 1973) are exactly matched to areas with heavy ECM Reelin immunostaining (Misaki *et al.*, 2004; present results). A mitral cell origin for the Reelin in these areas is further supported by the fact that some of them, such as the olfactory tuberculum and AOL, are

virtually devoid of local Reelin-expressing neurons (Figs 1E and 2A). An equivalent pattern is present in the cells of origin, axons and terminal neuropil of other long pathways. For example, entorhinal layer II and III cells express Reelin mRNA (Alcántara *et al.*, 1998; Haas *et al.*, 2000), their axons contain intra-axonal Reelin-ir particles (Fig. 7C–E), and their terminal neuropil in the CA and DG is selectively matched with a band of high ECM Reelin labeling (Fig. 7F). A similar situation might occur in some retino-mesencephalic projections (Fig. 9). The observed distribution of neuropil labeling in the superficial layers of the superior colliculus and the accessory optic nuclei, all of which receive direct retinal projections, suggests that some retinal ganglion cells secrete Reelin into their mesencephalic target fields. The presence of Reelin mRNA and protein in a population of retinal ganglion cells (Schiffmann *et al.*, 1997; Rice *et al.*, 2001; present results) adds support to this possibility. In other cases, the source of high local ECM Reelin levels appears to be located at a shorter distance. This was previously noted for the cerebellar granule cell axons that secrete Reelin in the ECM of the molecular layer (Miyata *et al.*, 1996; Pesold *et al.*, 1998; present results). Likewise, the neuropil labeling in isocortical sublayer Ia (Pesold *et al.*, 1998; Rodríguez *et al.*, 2000, 2002; Pérez-García *et al.*, 2001; Deguchi *et al.*, 2003; Roberts *et al.*, 2005; present results) might originate, at least in part, in the selective innervation of this sublayer by Martinotti cells (Wang *et al.*, 2004), most of which express Reelin in the adult isocortex (Alcántara *et al.*, 1998; Pesold *et al.*, 1998, 1999).

In summary, the available evidence is consistent with the possibility that Reelin accumulates in some neuropil areas distantly located from the cell bodies that actually synthesize the protein, and even in regions that do not contain any Reelin-expressing cell neurons. Future axon lesion experiments, or application of axonal transport blockers, could directly confirm the axonal flow of Reelin in some of these pathways, and also provide a measure of persistence/clearance of secreted Reelin.

Reelin-immunoreactive cell types in the forebrain

The morphology and distribution of the Reelin-ir interneurons in the isocortex, entorhinal cortex and hippocampus agree with previous observations in adult rodents (Ikeda & Terashima, 1997; Alcántara *et al.*, 1998; Drakew *et al.*, 1998; Pesold *et al.*, 1998, 1999; Haas *et al.*, 2000; Pérez-García *et al.*, 2001). In the hippocampus, all the labeled cells display interneuron morphology and co-localize GABA (Figs 5, and 7G and H). In the entorhinal cortex Reelin is present in both interneurons and pyramidal neurons of layers II–III (Fig. 7A and B). In the isocortex, Reelin is present in numerous interneurons in all layers, but also in a sizable population of non-GABAergic pyramidal cells in layer V. The latter observation is relevant because it supports the finding of low but consistent Reelin mRNA and protein levels in pyramidal cells by Pesold *et al.* (1998, 1999), in contrast to studies

FIG. 8. Reelin-like immunolabeling in the diencephalon. (A–C) Low-magnification views of coronal sections taken from the rostral pole of the thalamus (A, approximately at bregma -1.10), as well as from two other levels (B, bregma -1.80 mm; C, bregma -4.50 mm). Note in A the labeled neuronal somata in the anterodorsal (AD) and anterior paraventricular (PvA) thalamic nuclei, and in the nucleus of the stria medullaris (SMN). A Reelin-ir cell population located within the external medullary lamina is indicated by arrows. Despite its inconspicuous adult appearance, this neuron population is a remnant of the zona limitans intrathalamica of the embryo (Alcántara *et al.*, 1998). Note in C that numerous Reelin-ir neuronal somata are scattered throughout the dorsal lateral geniculate (DLG) and lateral posterior (LP) nuclei but are conspicuously absent from the ventrobasal (VB) and posterior (Po) thalamic groups. Large numbers of cells are labeled in the pretectal nuclei (APT, OPT), in the posterior hypothalamus (PH) and periaqueductal gray (PaG), as well as in the ventral lateral geniculate nuclei, particularly in its magnocellular part (VLGmc). The axons of the habenulo-interpeduncular tract (RB) are immunolabeled; by comparison, note the absence of labeling in the medial lemniscus (ML). (D) High-magnification view of the neuronal somata labeled in the AD thalamic nucleus. (E) High-magnification view of the labeled cells in the DLG. Note that compared with the image in D (at the same scale), the DLG cells are clearly smaller, consistent with the finding that they are GABAergic thalamic interneurons (Fig. 5). (F) Detail of the labeling in the olivary pretectal nucleus (OPT). Note that, in addition to its neuronal somata, the neuropil of OPT is heavily immunoreactive. (G) Labeling in the habenular complex. In addition to numerous somata, note the heavy labeling of some axon bundles of the habenulo-interpeduncular tract (arrow). There is dense neuropil labeling in a portion of the medial habenular nucleus (arrowheads). For other abbreviations, see List. Scale bars, 500 μ m (A–C and G); 20 μ m (D and E); 100 μ m (F).

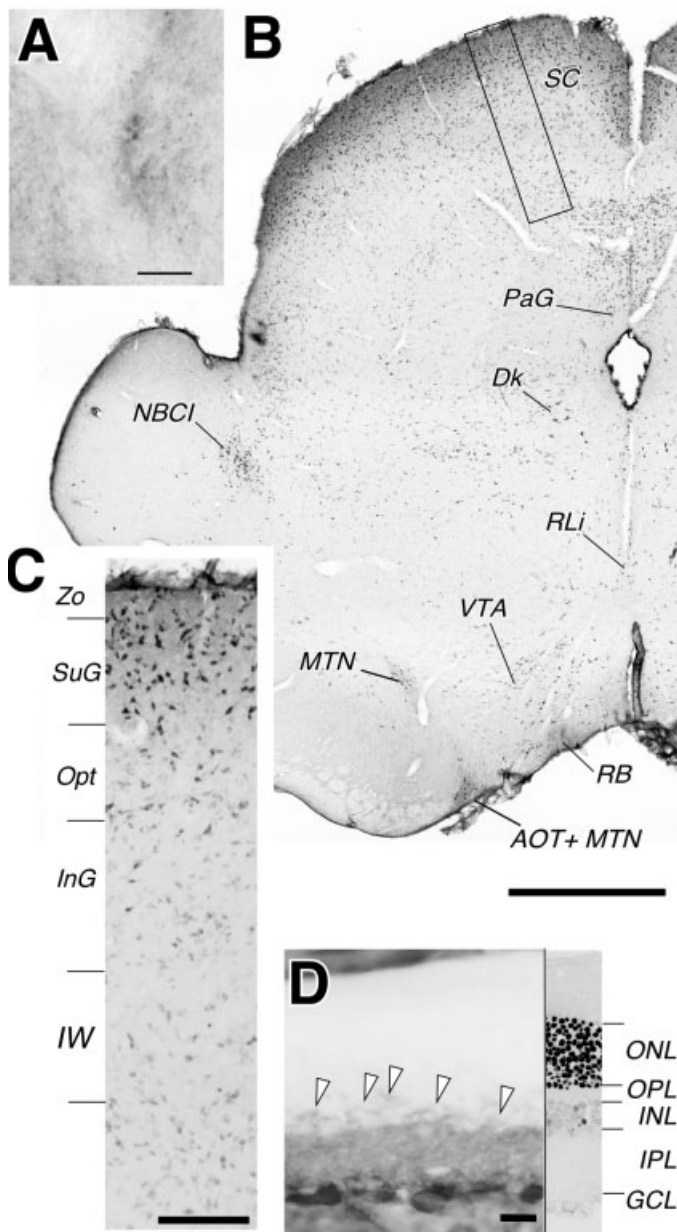


FIG. 9. Reelin-like immunolabeling in the mesencephalon and retina. (A–C) Labeling in rostral mesencephalon. The panoramic view of a coronal section (B) at the level of the superior colliculus shows numerous ReIn-ir cell somata and areas of neuropil labeling. There is also labeling in some axons of the habenulo-interpeduncular tract (RB); a high-magnification view of these axons is shown in A. The superior colliculus (SC) is conspicuously labeled. A more detailed view of its four superior layers is illustrated in C. Note that the most heavily stained somata are located in the stratum zonale (Zo) and stratum griseum superior (SuG). Note that, in addition, the neuropil is heavily immunoreactive in these two most superficial SC layers. Additional groups of ReIn-ir neurons are visible in the nucleus of the brachium of the inferior colliculus (NBCI), Darkewitsch (Dk) and raphe (RLi) nuclei. Note also the labeling in the medial terminal nucleus of the accessory optic tract and in the retinal fibers of the accessory optic tract (AOT, MTN). (D) Immunolabeling of a coronal section of the retina. For cytoarchitectonic reference, a strip from a parallel semithin section stained with toluidine blue is attached on the right side of the panel. Note the numerous ReIn-ir neuronal somata in the ganglion cell layer (GCL). There is also weak labeling in the cytoplasm of some cells in the inner nuclear layer (INL, arrowheads). A prominent band of neuropil immunolabeling delineates the internal plexiform layer (IPL). Scale bars, 10 μm (A); 1 mm (B); 100 μm (C).

that had concluded that in the isocortex only interneurons expressed or contained Reelin (Alcántara *et al.*, 1998; Pérez-García *et al.*, 2001). Specifically, Pesold and colleagues reported that about 30% of isocortical cells expressing Reelin mRNA were not GABAergic, and noted that some of them had pyramidal morphology. Our data (Figs 3, 5 and 6) confirm and extend these observations, showing that, in fact, a large population of non-GABAergic pyramidal cells in layer V of the isocortex contain Reelin. Interestingly, these rodent findings are in agreement with reports of Reelin in numerous isocortical pyramidal cells in adult primates, including humans (Rodríguez *et al.*, 2000; Martínez-Cerdeño *et al.*, 2002; Deguchi *et al.*, 2003; Roberts *et al.*, 2005).

Consistent with findings in adult carnivores (Martínez-Cerdeño *et al.*, 2003) and non-human primates (Martínez-Cerdeño *et al.*, 2002), numerous rat striatal neurons contain low Reelin levels (Fig. 2). The Reelin content of these neurons seems to decrease throughout adulthood. The most heavily labeled cells are preferentially located in the striosomal compartment. These findings are in agreement with reports of Reelin mRNA (Alcántara *et al.*, 1998) and protein (Nishikawa *et al.*, 1999) in postnatal rodent striatum, with a preferential localization in striosomes. Alcántara *et al.* (1998), however, did not detect Reelin mRNA in the adult mouse striatum; because the riboprobes used in the same experiments apparently did not detect low adult mRNA levels present in pyramidal cells of the adult isocortex (see above), it is possible that they also missed low Reelin mRNA levels in the striatum. Alternatively, our immunolabeling of striatal neurons may correspond to Reelin internalized in endosomes (D'Arcangelo *et al.*, 1999; Morimura *et al.*, 2005).

The present results show that several dorsal thalamic nuclei contain ReIn-ir cells. Labeled cells in the anterodorsal, paraventricular and anterior intralaminar must be projection neurons, because these nuclei lack intrinsic interneurons in rodents (Arcelli *et al.*, 1997). By contrast, the distribution, morphology and strict co-localization with GABA consistently indicate that ReIn-ir neurons in DLG and LP (Fig. 5) are the intrinsic interneurons known to exist in these nuclei of the rat thalamus (Ohara *et al.*, 1983; Arcelli *et al.*, 1997).

Reelin-containing cells are numerous in other diencephalic districts (Puelles & Rubenstein, 2003) such as the epithalamus, zona limitans intrathalamica (ZLI; Kitamura *et al.*, 1997), prethalamus and pretectum. It is interesting to note that, during development, the prethalamic eminence and ZLI derivatives express high levels of Reelin mRNA (Alcántara *et al.*, 1998). We show here that Reelin remains present in adult derivatives of these embryonic structures (Kitamura *et al.*, 1997; Alcántara *et al.*, 1998; Nakagawa & O'Leary, 2001; Hayes *et al.*, 2003) such as the ventral lateral geniculate nucleus, the intergeniculate leaflet, the neurons of the external medullary lamina, the ventral reuniens thalamic nucleus and some subnuclei of the hypothalamic paraventricular nucleus.

Comparative remarks

Adding to earlier reports in macaques and ferrets (Martínez-Cerdeño *et al.*, 2002, 2003), the present rat data reveal a conserved basic pattern of Reelin protein localization in equivalent neuron populations, axonal tracts and neuropil areas of the forebrain. Such a basic constancy lends relevance to differences in Reelin protein content observed in particular neuron populations between these species. This is the case, for example, of cortical pyramidal cells or thalamic cells. Reelin protein is present in virtually all isocortical pyramidal cells in macaques, in virtually all layer V pyramidal cells in rats but only in occasional layer V pyramids in ferrets. In macaques, subiculum and CA pyramidal cells are ReIn-ir, in rats only parasubiculum pyramidal

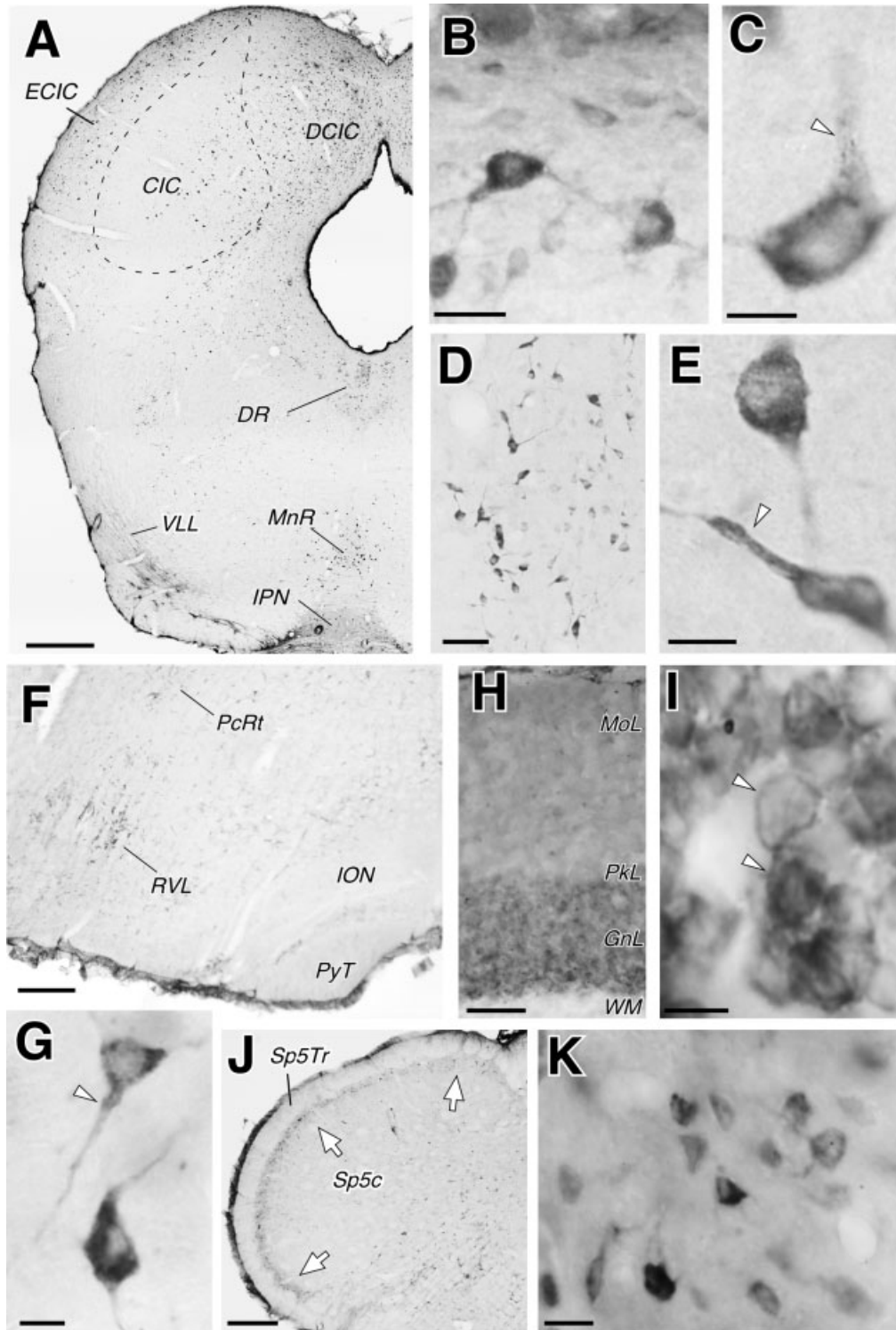


FIG. 10. Reelin-like immunolabeling in the hindbrain and cerebellum. (A) Coronal section at the level of the inferior colliculus. Note the abundant cell somata labeling in external cortex (ECIC) and dorsal cortex (DCIC) of the colliculus. (B) Immunolabeled cells and neuropil in ECIC. (C) Large multipolar cell of the DCIC. Note that, as observed in neurons throughout the brain, this neuron contains intracellular ReIn-ir clumps in the perikaryon and proximal dendrites (arrowhead). (D and E) Labeling in the medial raphe nucleus. Elongated particles are present within the dendrites and perikaryon of the neurons (arrowhead in E). (F) Labeling in the ventral medulla oblongata. A prominent group of ReIn-ir neurons are visible in the ventral lateral reticular nucleus (RVL). Note the absence of labeling in the inferior olivary nucleus (ION). (G) detail of two ReIn-ir neurons of the RVL. (H and I) Immunolabeling of the cerebellar cortex. Heavy neuropil immunolabeling is present throughout the molecular (MoL) layer. There is no labeling in the Purkinje cells (PkL), but virtually all the cells in the granule cell layer (GnL) are immunoreactive. An example of the cytoplasmic labeling of these granule cells is illustrated in I. (J and K) Immunoreactive neuronal somata and neuropil (arrows) in the superficial layer of the spinal trigeminal nucleus (Sp5c). K shows a high-magnification view of the small ReIn-ir neurons in this layer, amidst abundant extracellular immunolabeling. For other abbreviations, see List. Scale bars, 500 μ m (A and F); 20 μ m (B); 10 μ m (C, E, G and K); 50 μ m (D and H); 100 μ m (J); 5 μ m (I).

cells are Reelin-ir and no pyramidal cells are Reelin-ir in the CA or subiculum of ferrets. Likewise, in macaques and ferrets, large numbers of neurons throughout the thalamus contain Reelin, whereas, in rats, Reelin is found only in a limited number of cells of a few thalamic nuclei. Fossil and molecular genetic evidence indicates that rats and macaques diverged from a common ancestor about 80–90 million years ago while the ferret lineage split even earlier, around 90–100 million years ago (Murphy *et al.*, 2004). From an evolutionary perspective therefore the finding of fine-grained interspecies differences in expression and/or protein processing by some neuronal populations is unsurprising, all the more so if one compares forebrain structures that have independently expanded in each lineage (Striedter, 2004). In addition, the comparison between the three species shows that Reelin is most abundant and widely distributed in the primate brain; this seems remarkable in view of mounting evidence that Reelin regulates the synaptic substrates for learning and memory (D'Arcangelo, 2005a).

Supplementary material

The following supplementary material may be found on <http://www.blackwell-synergy.com>

Fig. S1. Immunolabeling controls.

Fig. S2. Specificity of the Reelin immunolabeling.

Acknowledgements

We wish to thank Dr Mario Vallejo, Instituto de Investigaciones Biomédicas CSIC, Madrid, for his valuable help with the Western blot analysis, Dr Masaharu Ogawa RIKEN, Japan, for the gift of the CR-50 antibody, Dr Jose Antonio del Rio, Parc Científic-Barcelona University, for the supernatants of Reelin-transfected cells, and Carol Warren for linguistic assistance. Financial support was received from Spanish Ministry of Education and Science (Grant BFI 2002/04674), Comunidad de Madrid (Grant 08.05/0002/2001) and 'Eugenio Rodríguez Pascual' Foundation, Madrid. M.J.G. is the recipient of an MEC-FPU Predoctoral Fellowship.

Abbreviations

ABL, basal and lateral amygdaloid nuclei; AC, anterior commissure; ACo, cortical amygdaloid nucleus; ACP, anterior commissure, posterior branch; AD, anterodorsal thalamic nucleus; AMe, medial amygdaloid nucleus; AOB, accessory olfactory bulb; AOL, anterior olfactory nucleus, lateral division; AOT, accessory optic tract; APT, anterior pretectal nucleus; Au1, primary auditory cortex; AV, anteroventral thalamic nucleus; BST, bed nucleus of the stria terminalis; CA1, Ammon's horn sector 1; CA3, Ammon's horn sector 3; CeL, centralis lateralis thalamic nucleus; CIC, inferior colliculus, central nucleus; CM, centralis medialis thalamic nucleus; CPu, caudate-putamen; DCIC, inferior colliculus, dorsal cortex; DG, dentate gyrus; Dk, Darkewitsch's nucleus; DLG, dorsal lateral geniculate thalamic nucleus; DR, dorsal raphe nucleus; ECIC, inferior colliculus, external cortex; End, endopyriform nucleus; EPL, external plexiform layer of the main olfactory bulb; Fx, fornix; GCL, ganglion cell layer; GIL, glomerular layer of the main olfactory bulb; GnL, granule cell layer of the cerebellar cortex; GnL, granular layer of main olfactory bulb; GP, globus pallidus; GrDG, granule cell layer of the dentate gyrus; HDB, diagonal band nuclei, horizontal limb; HF, hippocampal fissure; Hi, hilus layer of the dentate gyrus; Iam, interanteromedial thalamic nucleus; ICj, cell islands of calleja; InG, intermediate gray stratum of the superior colliculus; INL, inner nuclear layer; ION, inferior olivary nucleus; IPL, internal plexiform layer; IPN, interpeduncular nucleus; LEA, lateral entorhinal area; LHb, lateral habenular nucleus; LMol, stratum lacunosum-moleculare, Ammon's horn; LOT, lateral olfactory tract; LP, lateralis posterior thalamic nucleus; LPO, lateral preoptic area; LSpI, lateral septal nucleus, intermediate subnucleus; LSpL, lateral septal nucleus, lateral subnucleus; M, mitral cell layer of the main olfactory bulb; McPo, magnocellular preoptic nucleus; MEA, medial entorhinal area; MHb, medial habenular nucleus; ML, medial lemniscus; MnR, raphe magnus nucleus; MOB, main olfactory bulb; Mol, molecular layer of the dentate gyrus; MoL, molecular layer of the cerebellar cortex; MPo, medial preoptic area; MSP,

medial septal nucleus; MTN, medial terminal accessory optic nucleus; NCBI, nucleus of the brachium of the inferior colliculus; ON, olfactory nerve layer of the main olfactory bulb; ONL, outer nuclear layer of the retina; OPL, outer plexiform layer of the retina; OPT, olivary pretectal nucleus; Opt, optic stratum of the superior colliculus; PaDC, paraventricular hypothalamic nucleus, dorsal cap; PaG, periaqueductal gray; PaLM, paraventricular hypothalamic nucleus, lateral magnocellular part; PaSb, parasubiculum; Pc, paracentral thalamic nucleus; PcRt, parvocellular reticular nucleus; PerC, perirhinal cortex; PH, posterior hypothalamic area; PkL, purkinje cell layer of the cerebellar cortex; Po, posterior thalamic nucleus; PoDG, polymorph layer of the dentate gyrus; Ppir, prepyriform cortex; ProC, prothalamal cortex; PrS, presubiculum; Pt, paratenial thalamic nucleus; PvA, anterior paraventricular thalamic nucleus; PVP, posterior paraventricular thalamic nucleus; PyT, pyramidal tract; Py, stratum pyramidale, Ammon's horn; Rad, stratum radiatum, Ammon's horn; RB, retroflex bundle (habenulo-interpeduncular tract); Rli, raphe linearis nucleus; RVL, rostroventrolateral reticular nucleus; S1, somatosensory area 1, parietal isocortex; Sb, subiculum; SC, superior colliculus; SM, stria medullaris thalami; SMN, nucleus of the stria medullaris thalami; Sp5c, caudal portion of the spinal trigeminal nucleus; Sp5Tr, spinal tract of the trigeminal nucleus; ST, stria terminalis; SuG, superficial gray stratum of the superior colliculus; TuO, olfactory tubercle; VLGmc, ventral lateral geniculate nucleus, magnocellular part; VLGpc, ventral lateral geniculate nucleus, parvocellular part; VLL, ventral lateral lemniscus nucleus; VP, ventral pallidum; VPM, medial ventroposterior thalamic nucleus; VRe, ventral reunions nucleus; VTA, ventral tegmental area; ZI, zona incerta; ZLI, zona limitans intrathalamica; DAB, diaminebenzidine; ECM, extracellular matrix; GABA, gamma-aminobutyric acid; ISH, in situ hybridization; NMDAR, *N*-methyl-D-aspartate receptor; ReIn-ir, Reelin-immunoreactive.

References

- Alcántara, S., Ruiz, M., D'Arcangelo, G., Ezan, F., de Lecea, L., Curran, T., Sotelo, C. & Soriano, E. (1998) Regional and cellular patterns of reelin mRNA expression in the forebrain of the developing and adult mouse. *J. Neurosci.*, **18**, 7779–7799.
- Amaral, D.G. & Witter, M.P. (1994) Hippocampal formation. In Paxinos, G. (Ed.), *The Rat Nervous System*, 2nd edn. Academic Press, San Diego, pp. 443–493.
- Andersen, O.M., Benhayon, D., Curran, T. & Willnow, T.E. (2003) Differential binding of ligands to the apolipoprotein E receptor 2. *Biochemistry*, **42**, 9355–9364.
- Arcelli, P., Frassoni, C., Regondi, M.C., De Biasi, S. & Spreafico, R. (1997) GABAergic neurons in mammalian thalamus: a marker of thalamic complexity? *Brain Res. Bull.*, **42**, 27–37.
- Beffert, U., Weeber, E.J., Durudas, A., Qiu, S., Masidulis, I., Sweatt, D., Li, W.-P., Adelman, G., Frotscher, M., Hammer, R.E. & Herz, J. (2005) Modulation of synaptic plasticity and memory by reelin involves differential splicing of the lipoprotein receptor Apoer2. *Neuron*, **47**, 567–579.
- Benhayon, D., Magdaleno, S. & Curran, T. (2003) Binding of purified Reelin to ApoER2 and VLDLR mediates tyrosine phosphorylation of Disabled-1. *Brain Res. Mol. Brain Res.*, **112**, 33–45.
- Berardi, N., Pizzorusso, T. & Maffei, L. (2004) Extracellular matrix and visual cortical plasticity: freeing the synapse. *Neuron*, **44**, 905–908.
- de Bergeyck, V., Naerhuyzen, B., Goffinet, A.M. & Lambert de Rouvroit, C. (1998) A panel of monoclonal antibodies against reelin, the extracellular matrix protein defective in reeler mutant mice. *J. Neurosci. Methods*, **82**, 17–24.
- Cameron, P., Mundigl, O. & De Camilli, P. (1993) Traffic of synaptic proteins in polarized and nonpolarized cells. *J. Cell Sci. Suppl.*, **17**, 93–100.
- Chen, Y., Beffert, U., Ertunc, M., Tang, T.-S., Kavalali, E.T., Bezprozvanny, I. & Herz, J. (2005) Reelin modulates de NMDA receptor activity in cortical neurons. *J. Neurosci.*, **25**, 8209–8216.
- D'Arcangelo, G. (2005a) Apoer2: a reelin receptor to remember. *Neuron*, **47**, 471–473.
- D'Arcangelo, G. (2005b) The reeler mouse: anatomy of a mutant. In: Dhossche, D.M. (Ed.), *International Review of Neurobiology*, **71**, the *Neurobiology of Autism*. Elsevier, San Diego, pp. 383–417.
- D'Arcangelo, G., Homayouni, R., Keshvara, L., Rice, D.S., Sheldon, M. & Curran, T. (1999) Reelin is a ligand for lipoprotein receptors. *Neuron*, **24**, 471–479.
- D'Arcangelo, G., Miao, G.G., Chen, S.C., Soares, H.D., Morgan, J.I. & Curran, T. (1995) A protein related to extracellular matrix proteins deleted in the mouse mutant reeler. *Nature*, **374**, 719–723.

- D'Arcangelo, G., Nakajima, K., Miyata, T., Ogawa, M., Mikoshiba, K. & Curran, T. (1997) Reelin is a secreted glycoprotein recognized by the CR-50 monoclonal antibody. *J. Neurosci.*, **17**, 23–31.
- De Camilli, P., Moretti, M., Donini, S.D., Walter, U. & Lohmann, S.M. (1986) Heterogeneous distribution of the cAMP receptor protein RII in the nervous system, evidence for its intracellular accumulation on microtubules, microtubule-organizing centers and in the area of the Golgi complex. *J. Cell Biol.*, **103**, 189–203.
- Deguchi, K., Inoue, K., Avila, W.E., Lopez-Terrada, D., Antalfy, B.A., Quattrocchi, C.C., Sheldon, M., Mikoshiba, K., D'Arcangelo, G. & Armstrong, D.L. (2003) Reelin and disabled-1 expression in developing and mature human cortical neurons. *J. Neuropathol. Exp. Neurol.*, **62**, 676–684.
- Del Rio, J.A., Heimrich, B., Borrell, V., Forster, E., Drakew, A., Alcántara, S., Nakajima, K., Miyata, T., Ogawa, M., Mikoshiba, K., Derer, P., Frotscher, M. & Soriano, E. (1997) A role for Cajal-Retzius cells and reelin in the development of hippocampal connections. *Nature*, **385**, 70–74.
- Deller, T., Adelman, G., Nitsch, R. & Frotscher, M. (1996) The alvear pathway of the rat hippocampus. *Cell Tissue Res.*, **286**, 293–303.
- Derer, P., Derer, M. & Goffinet, A. (2001) Axonal secretion of Reelin by Cajal-Retzius cells: evidence from comparison of normal and Reln (Orl) mutant mice. *J. Comp. Neurol.*, **440**, 136–143.
- Dityatev, A. & Schachner, M. (2003) Extracellular matrix molecules and synaptic plasticity. *Nat. Rev. Neurosci.*, **4**, 456–468.
- Dong, E., Caruncho, H., Liu, W.S., Smalheiser, N.R., Grayson, D.R., Costa, E. & Guidotti, A. (2003) A reelin-integrin receptor interaction regulates Arc mRNA translation in synaptoneuroosomes. *Proc. Natl Acad. Sci. USA*, **100**, 5479–5484.
- Drakew, A., Frotscher, M., Deller, T., Ogawa, M. & Heimrich, B. (1998) Developmental distribution of a reeler gene-related antigen in the rat hippocampal formation visualized by CR-50 immunocytochemistry. *Neuroscience*, **82**, 1079–1086.
- Dulabon, L., Olson, E.C., Taglienti, M.G., Eisenhuth, S., McGrath, B., Walsh, C.A., Kreidberg, J.A. & Anton, E.S. (2000) Reelin binds alpha3beta1 integrin and inhibits neuronal migration. *Neuron*, **27**, 33–44.
- Femino, A.M., Fay, F.S., Fogarty, K. & Singer, R.H. (1998) Visualization of single RNA transcripts in situ. *Science*, **280**, 585–590.
- Geinisman, Y., de Toledo-Morrell, L., Morrell, F., Persina, I.S. & Rossi, M. (1992) Structural synaptic plasticity associated with the induction of long-term potentiation is preserved in the dentate gyrus of aged rats. *Hippocampus*, **2**, 445–456.
- Gygi, S.P., Rochon, Y., Franza, B.R. & Aebersold, R. (1999) Correlation between protein and mRNA abundance in yeast. *Mol. Cell Biol.*, **19**, 1720–1730.
- Haas, C.A., Deller, T., Krsnik, Z. & Tielsch, A., Woods, A. & Frotscher, M. (2000) Entorhinal cortex lesion does not alter reelin messenger RNA expression in the dentate gyrus of young and adult rats. *Neuroscience*, **97**, 25–31.
- Haas, C.A., Dudeck, O., Kirsch, M., Huszka, C., Kann, G., Pollak, S., Zentner, J. & Frotscher, M. (2002) Role for reelin in the development of granule cell dispersion in temporal lobe epilepsy. *J. Neurosci.*, **22**, 5797–5802.
- Hack, I., Bancila, M., Loulier, K., Carroll, P. & Cremer, H. (2002) Reelin is a detachment signal in tangential chain-migration during postnatal neurogenesis. *Nat. Neurosci.*, **5**, 939–945.
- Hayes, S.G., Murray, K.D. & Jones, E.G. (2003) Two epochs in the development of gamma-aminobutyric acidergic neurons in the ferret thalamus. *J. Comp. Neurol.*, **463**, 45–65.
- Ignatova, N., Sincic, C.J. & Goffinet, A.M. (2004) Characterization of the various forms of the Reelin protein in the cerebrospinal fluid of normal subjects and in neurological diseases. *Neurobiol. Dis.*, **15**, 326–330.
- Ikeda, Y. & Terashima, T. (1997) Expression of reelin, the gene responsible for the reeler mutation, in embryonic development and adulthood in the mouse. *Dev. Dyn.*, **210**, 157–172.
- Impagnatiello, F., Guidotti, A.R., Pesold, C., Dwivedi, Y., Caruncho, H., Pisu, M.G., Uzunov, D.P., Smalheiser, N.R., Davis, J.M., Pandey, G.N., Pappas, G.D., Tueting, P., Sharma, R.P. & Costa, E. (1998) A decrease of reelin expression as a putative vulnerability factor in schizophrenia. *Proc. Natl Acad. Sci. USA*, **95**, 15718–15723.
- Jossin, Y. (2004) Neuronal migration and the role of reelin during early development of the cerebral cortex. *Mol. Neurobiol.*, **30**, 225–251.
- Jossin, Y., Ignatova, N., Hiesberger, T., Herz, J., Lambert de Rouvroit, C. & Goffinet, A.M. (2004) The central fragment of Reelin, generated by proteolytic processing in vivo, is critical to its function during cortical plate development. *J. Neurosci.*, **24**, 514–521.
- Kitamura, K., Miura, H., Yanazawa, M., Miyashita, T. & Kato, K. (1997) Expression patterns of Brx1 (Rieg gene), Sonic hedgehog, Nkx2.2, Dlx1 and Arx during zona limitans intrathalamica and embryonic ventral lateral geniculate nuclear formation. *Mech. Dev.*, **67**, 83–96.
- Klintonova, A.Y. & Greenough, W.T. (1999) Synaptic plasticity in cortical systems. *Curr. Opin. Neurobiol.*, **9**, 203–208.
- Kubo, K., Mikoshiba, K. & Nakajima, K. (2002) Secreted Reelin molecules form homodimers. *Neurosci. Res.*, **43**, 381–388.
- Lacor, P.N., Grayson, D.R., Auta, J., Sugaya, I., Costa, E. & Guidotti, A. (2000) Reelin secretion from glutamatergic neurons in culture is independent from neurotransmitter regulation. *Proc. Natl Acad. Sci. USA*, **97**, 3556–3561.
- Lambert de Rouvroit, C., de Bergeyck, V., Cortvrindt, C., Bar, I., Eeckhout, Y. & Goffinet, A.M. (1999) Reelin, the extracellular matrix protein deficient in reeler mutant mice, is processed by a metalloproteinase. *Exp. Neurol.*, **156**, 214–217.
- Martínez-Cerdeño, V. & Clascá, F. (2002) Reelin immunoreactivity in the adult neocortex: a comparative study in rodents, carnivores, and non-human primates. *Brain Res. Bull.*, **57**, 485–488.
- Martínez-Cerdeño, V., Galazo, M.J. & Clascá, F. (2002) Reelin immunoreactivity in the adult primate brain. Intracellular localization in projecting and local circuit neurons of the cerebral cortex, hippocampus and subcortical regions. *Cereb. Cortex*, **12**, 1298–1311.
- Martínez-Cerdeño, V., Galazo, M.J. & Clascá, F. (2003) Reelin-immunoreactive neurons, axons, and neuropil in the adult ferret brain: evidence for axonal secretion of reelin in long axonal pathways. *J. Comp. Neurol.*, **463**, 92–116.
- McKay, B.E., Molineux, M.L. & Turner, R.W. (2004) Biotin is endogenously expressed in select regions of the rat central nervous system. *J. Comp. Neurol.*, **473**, 86–96.
- Misaki, K., Kikkawa, S. & Terashima, T. (2004) Reelin-expressing neurons in the anterior commissure and corpus callosum of the rat. *Brain Res. Dev. Brain Res.*, **148**, 89–96.
- Miyata, T., Nakajima, K., Aruga, J., Takahashi, S., Ikenaka, K., Mikoshiba, K. & Ogawa, M. (1996) Distribution of a reeler gene-related antigen in the developing cerebellum. An immunohistochemical study with an allogeneic antibody CR-50 on normal and reeler mice. *J. Comp. Neurol.*, **372**, 215–228.
- Morimura, T., Hattori, M., Ogawa, M. & Mikoshiba, K. (2005) Disabled-1 regulates the intracellular trafficking of reelin receptors. *J. Biol. Chem.*, **280**, 16901–16908.
- Murphy, W.J., Pevzner, P.A. & O'Brien, S.J. (2004) Mammalian phylogenomics comes of age. *Trends Genet.*, **20**, 631–639.
- Nakagawa, Y. & O'Leary, D.D. (2001) Combinatorial expression patterns of LIM-homeodomain and other regulatory genes parcellate developing thalamus. *J. Neurosci.*, **21**, 2711–2725.
- Nakajima, K., Mikoshiba, K., Miyata, T., Kudo, C. & Ogawa, M. (1997) Disruption of hippocampal development in vivo by CR-50 mAb against reelin. *Proc. Natl Acad. Sci. USA*, **94**, 8196–8201.
- Nishikawa, S., Goto, S., Hamasaki, T., Ogawa, M. & Ushio, Y. (1999) Transient and compartmental expression of the reeler gene product reelin in the developing rat striatum. *Brain Res.*, **850**, 244–248.
- Niu, S., Renfro, A., Quattrocchi, C.C., Sheldon, M. & D'Arcangelo, G. (2004) Reelin promotes hippocampal dendrite development through the VLDLR/ApoER2-Dab1 pathway. *Neuron*, **41**, 71–84.
- Ogawa, M., Miyata, T., Nakajima, K., Yagyu, K., Seike, M., Ikenaka, K., Yamamoto, H. & Mikoshiba, K. (1995) The reeler gene-associated antigen on Cajal-Retzius neurons is a crucial molecule for laminar organization of cortical neurons. *Neuron*, **14**, 899–912.
- Ohara, P.T., Lieberman, A.R., Hunt, S.P. & Wu, J.Y. (1983) Neural elements containing glutamic acid decarboxylase (GAD) in the dorsal lateral geniculate nucleus of the rat; immunohistochemical studies by light and electron microscopy. *Neuroscience*, **8**, 189–211.
- Oray, S., Majewska, A. & Sur, M. (2004) Dendritic spine dynamics are regulated by monocular deprivation and extracellular matrix degradation. *Neuron*, **44**, 1021–1030.
- Pappas, G.D., Kriho, V., Liu, W.S., Tremolizzo, L., Lugli, G. & Larson, J. (2003) Immunocytochemical localization of reelin in the olfactory bulb of the heterozygous reeler mouse: an animal model for schizophrenia. *Neurosci. Res.*, **25**, 819–830.
- Pappas, G.D., Kriho, V. & Pesold, C. (2001) Reelin in the extracellular matrix and dendritic spines of the cortex and hippocampus: a comparison between wild type and heterozygous reeler mice by immunoelectron microscopy. *J. Neurocytol.*, **30**, 413–425.
- Paxinos, G. & Watson, C. (1998) *The Rat Brain in Stereotaxic Coordinates*. Academic Press, San Diego.
- Pérez-García, C.G., González-Delgado, F.J., Suárez-Sola, M.L., Castro-Fuentes, R., Martín-Trujillo, J.M., Ferrer-Torres, R. & Meyer, G. (2001)

- Reelin-immunoreactive neurons in the adult vertebrate pallium. *J. Chem. Neuroanat.*, **21**, 41–51.
- Pesold, C., Impagnatiello, F., Pisu, M.G., Uzunov, D.P., Costa, E., Guidotti, A. & Caruncho, H.J. (1998) Reelin is preferentially expressed in neurons synthesizing gamma-aminobutyric acid in cortex and hippocampus of adult rats. *Proc. Natl Acad. Sci. USA*, **95**, 3221–3226.
- Pesold, C., Liu, W.S. & Guidotti, A., Costa, E. & Caruncho, H.J. (1999) Cortical bitufted, horizontal, and Martinotti cells preferentially express and secrete reelin into perineuronal nets, nonsynaptically modulating gene expression. *Proc. Natl Acad. Sci. USA*, **96**, 3217–3222.
- Prensa, L. & Parent, A. (2001) The nigrostriatal pathway in the rat. A single-axon study of the relationship between dorsal and ventral tier nigral neurons and the striosome/matrix striatal compartments. *J. Neurosci.*, **21**, 7247–7260.
- Price, J.L. (1973) An autoradiographic study of complementary laminar patterns of termination of afferent fibers to the olfactory cortex. *J. Comp. Neurol.*, **150**, 87–108.
- Puelles, L. & Rubenstein, J.L. (2003) Forebrain gene expression domains and the evolving prosomeric model. *Trends Neurosci.*, **26**, 469–476.
- Quattrocchi, C.C., Wannenes, F., Persico, A.M., Ciafre, S.A., D'Arcangelo, G., Farace, M.G. & Keller, F. (2002) Reelin is a serine protease of the extracellular matrix. *J. Biol. Chem.*, **277**, 303–309.
- Rice, D.S., Nusinowitz, S., Azimi, A.M., Martínez, A., Soriano, E. & Curran, T. (2001) The reelin pathway modulates the structure and function of retinal synaptic circuitry. *Neuron*, **31**, 929–941.
- Roberts, R.C., Xu, L., Roche, J.K. & Kirkpatrick, B. (2005) Ultrastructural localization of reelin in the cortex in post-mortem human brain. *J. Comp. Neurol.*, **482**, 294–308.
- Rodríguez, M.A., Pesold, C., Liu, W.S., Kriho, V., Guidotti, A., Pappas, G.D. & Costa, E. (2000) Colocalization of integrin receptors and reelin in dendritic spine postsynaptic densities of adult nonhuman primate cortex. *Proc. Natl Acad. Sci. USA*, **97**, 3550–3555.
- Rodríguez, M.A., Caruncho, H.J., Costa, E., Pesold, C., Liu, W.S. & Guidotti, A. (2002) In Patas monkey, glutamic acid decarboxylase-67 and reelin mRNA coexpression varies in a manner dependent on layers and cortical areas. *J. Comp. Neurol.*, **451**, 279–288.
- Saez-Valero, J., Costell, M., Sjogren, M., Andreasen, N., Blennow, K. & Luque, J.M. (2003) Altered levels of cerebrospinal fluid reelin in frontotemporal dementia and Alzheimer's disease. *J. Neurosci. Res.*, **72**, 132–136.
- Sakakibara, S., Misaki, K. & Terashima, T. (2003) Cytoarchitecture and fiber pattern of the superior colliculus are disrupted in the Shaking Rat Kawasaki. *Brain Res. Dev. Brain Res.*, **141**, 1–13.
- Sanada, K., Gupta, A. & Tsai, L.H. (2004) Disabled-1-regulated adhesion of migrating neurons to radial glial fiber contributes to neuronal positioning during early corticogenesis. *Neuron*, **42**, 197–211.
- Saper, C.B. & Sawchenko, P.E. (2003) Magic peptides, magic antibodies: guidelines for appropriate controls for immunohistochemistry. *J. Comp. Neurol.*, **465**, 161–163.
- Schiffmann, S.N., Bernier, B. & Goffinet, A.M. (1997) Reelin mRNA expression during mouse brain development. *Eur. J. Neurosci.*, **9**, 1055–1071.
- Schmid, R.S., Jo, R., Shelton, S., Kreidberg, J.A. & Anton, E.S. (2005) Reelin, integrin and Dab1 interactions during embryonic cerebral cortical development. *Cereb. Cortex*, **15**, 1632–1636.
- Sefton, A.J. & Dreher, B. (1994) Visual System. In: Paxinos, G. (Ed.), *The Rat Nervous System*, 2nd edn. Academic Press, San Diego, pp. 833–898.
- Shi, S.R., Cote, R.J. & Taylor, C.R. (2001) Antigen retrieval techniques: current perspectives. *J. Histochem. Cytochem.*, **49**, 931–937.
- Sinagra, M., Verrier, D., Frankova, D., Korwek, K.M., Blahos, J., Weeber, E.J., Manzoni, O.L. & Chavis, P. (2005) Reelin, very-low-density lipoprotein receptor, and apolipoprotein E receptor 2 control somatic NMDA receptor composition during hippocampal maturation in vitro. *J. Neurosci.*, **25**, 6127–6136.
- Smalheiser, N.R., Costa, E., Guidotti, A., Impagnatiello, F., Auta, J., Lacor, P., Kriho, V. & Pappas, G.D. (2000) Expression of reelin in adult mammalian blood, liver, pituitary pars intermedia, and adrenal chromaffin cells. *Proc. Natl Acad. Sci. USA*, **97**, 1281–1286.
- Speel, E.J., Hopman, A.H. & Komminoth, P. (1999) Amplification methods to increase the sensitivity of in situ hybridization: play card(s). *J. Histochem. Cytochem.*, **47**, 281–288.
- Strasser, V., Fasching, D., Hauser, C., Mayer, H. & Bock, H.H., Hiesberger, T., Herz, J., Weeber, E.J., Sweatt, J.D., Pramatarova, A., Howell, B., Schneider, W.J. & Nimpf, J. (2004) Receptor clustering is involved in Reelin signaling. *Mol. Cell Biol.*, **24**, 1378–1386.
- Striedter, G.F. (2004) *Principles of Brain Evolution*. Sinauer, Sunderland, MA.
- Tian, Q., Stepaniants, S.B., Mao, M., Weng, L., Feetham, M.C., Doyle, M.J., Yi, E.C., Dai, H., Thorsson, V., Eng, J., Goodlett, D., Berger, J.P., Gunter, B., Linseley, P.S., Stoughton, R.B., Aebersold, R., Collins, S.J., Hanlon, W.A. & Hood, L.E. (2004) Integrated genomic and proteomic analyses of gene expression in mammalian cells. *Mol. Cell Proteomics*, **3**, 960–969.
- Tissir, F. & Goffinet, A.M. (2003) Reelin and brain development. *Nat. Rev. Neurosci.*, **4**, 496–505.
- Utsunomiya-Tate, N., Kubo, K., Tate, S., Kainosho, M., Katayama, E., Nakajima, K. & Mikoshiba, K. (2000) Reelin molecules assemble together to form a large protein complex, which is inhibited by the function-blocking CR-50 antibody. *Proc. Natl. Acad. Sci. USA*, **97**, 9729–9734.
- Wang, Y., Toledo-Rodríguez, M., Gupta, A., Wu, C., Silberberg, G., Luo, J. & Markram, H. (2004) Anatomical, physiological and molecular properties of Martinotti cells in the somatosensory cortex of the juvenile rat. *J. Physiol.*, **561**, 65–90.
- Weeber, E.J., Beffert, U., Jones, C., Christian, J.M., Forster, E., Sweatt, J.D. & Herz, J. (2002) Reelin and ApoE receptors cooperate to enhance hippocampal synaptic plasticity and learning. *J. Biol. Chem.*, **277**, 39944–39952.
- Weeks, A.C., Ivanko, T.L., Leboutillier, J.C., Racine, R.J. & Petit, T.L. (1999) Sequential changes in the synaptic structural profile following long-term potentiation in the rat dentate gyrus. I. The intermediate maintenance phase. *Synapse*, **31**, 97–107.
- Yuste, R. & Bonhoeffer, T. (2001) Morphological changes in dendritic spines associated with long-term synaptic plasticity. *Annu. Rev. Neurosci.*, **24**, 1071–1089.
- Zhao, S., Chai, X., Forster, E. & Frotscher, M. (2004) Reelin is a positional signal for the lamination of dentate granule cells. *Development*, **131**, 5117–5125.